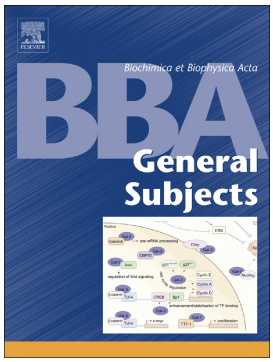

Genetically encoded fluorescent indicators for live cell pH imaging

Vladimir I. Martynov, Alexey A. Pakhomov, Igor E. Deyev, Alexander G. Petrenko

PII: S0304-4165(18)30301-5
DOI: doi:10.1016/j.bbagen.2018.09.013
Reference: BBAGEN 29216

To appear in: *BBA - General Subjects*

Received date: 9 July 2018
Revised date: 17 September 2018
Accepted date: 17 September 2018

Please cite this article as: Vladimir I. Martynov, Alexey A. Pakhomov, Igor E. Deyev, Alexander G. Petrenko , Genetically encoded fluorescent indicators for live cell pH imaging. Bbagen (2018), doi:10.1016/j.bbagen.2018.09.013

Genetically encoded fluorescent indicators for live cell pH imaging

Vladimir I. Martynov*, Alexey A. Pakhomov, Igor E. Deyev, Alexander G. Petrenko

Shemyakin–Ovchinnikov Institute of Bioorganic Chemistry, Russian Academy of Sciences.

***Corresponding author at:** Laboratory of Molecular Theranostics in Shemyakin–Ovchinnikov Institute of Bioorganic Chemistry,

Address for Correspondence: Vladimir I. Martynov

Miklukho-Maklaya St., 16/10, Moscow, 117997, Russia

Email: vimart@list.ru

Abstract

Background: Intracellular pH underlies most cellular processes. There is emerging evidence of a pH-signaling role in plant cells and microorganisms. Dysregulation of pH is associated with human diseases, such as cancer and Alzheimer's disease.

Scope of review: In this review, we attempt to provide a summary of the progress that has been made in the field during the past two decades. First, we present an overview of the current state of the design and applications of fluorescent protein (FP)-based pH indicators. Then, we turn our attention to the development and applications of hybrid pH sensors that combine the capabilities of non-GFP fluorophores with the advantages of genetically encoded tags. Finally, we discuss recent advances in multicolor pH imaging and the applications of genetically encoded pH sensors in multiparameter imaging.

Major conclusions: Genetically encoded pH sensors have proven to be indispensable noninvasive tools for selective targeting to different cellular locations. Although a variety of genetically encoded pH sensors have been designed and applied at the single cell level, there is still much room for improvements and future developments of novel powerful tools for pH imaging. Among the most pressing challenges in this area is the design of brighter redshifted sensors for tissue research and whole animal experiments.

General significance: The design of precise pH measuring instruments is one of the important goals in cell biochemistry and may give rise to the development of new powerful diagnostic tools for various diseases.

Keywords:

Biosensor; pH; Fluorescence; Ratiometric sensor; pH imaging; Microscopy

Abbreviations:

FP, fluorescent protein; avGFP, green fluorescent protein from *Aequorea victoria*; FRET, Förster resonance energy transfer; wt, wild-type; ESPT, excited state proton transfer; pHi, intracellular pH; EGFP, enhanced GFP; ECFP, enhanced cyan fluorescent protein; EYFP, enhanced yellow fluorescent protein; FLIM, fluorescence lifetime imaging microscopy; hCNT3, human nucleoside transport protein; mRFP, a monomeric mutant of the red fluorescent protein (DsRed) from *Discosoma* sp.; VGLUT1, vesicular glutamate transporter; mTangerine, mNectarine, mStrawberry, mCherry, mOrange, monomeric mutant FPs from the so-called mFruits series derived from mRFP.

1. Introduction

In live systems, pH controls many biochemical events, and pH alterations strongly affect cell function, growth, and division. pH is maintained within a sufficiently narrow interval of 7.1–7.2 and is regulated by membrane proton pumps and transporters whose activity is modulated by pH sensors [1]. Dysregulation of pH is often associated with human diseases, such as cancer [2-4] and Alzheimer's disease [5], and the ability of tumor cells to metastasize is dependent on the intracellular and extracellular pH [6]. A characteristic feature of eukaryotic cells is the compartmentalization of the intracellular space that enables different biochemical processes to be realized in different compartments. Most organelles have their individual pH value, associated with specific biochemical reactions that take place in their compartments. For example, maintenance of the lumenal pH in organelles of the secretory pathway is required for proper sorting and proteolytic processing of prohormones. Even small pH differences of < 0.5 pH units can alter prohormone processing [7].

Given the important role of pH in cell biochemistry, it is essential to obtain precise pH measuring instruments enabling spatial and temporal imaging of pH dynamics. There are a number of methods to measure pH including electrochemical [8], photoelectrochemical [9], surface-enhanced Raman spectroscopy [10, 11], optical [12] and some others. Among these, fluorescence microscopy is a method of preferred choice by cell biologists owing to its high sensitivity and excellent spatiotemporal resolution, rapid response, the possibility of experimentation at the molecular level and nondestructive detection. Today, a wide array of fluorescent pH probes is available for the use in fluorescence microscopy. These fluorophores include a group of nanomaterial-based probes, such as semiconductor quantum dots [13], gold nanoparticles [14], carbon nanomaterials [15, 16] and silica nanoparticles [17]. Another group comprises organic-inorganic nanocomposite-based probes [18-20]. There is also an extended group of small organic fluorescent molecules. These topics were recently discussed in several excellent reviews, to which the interested reader is referred [21, 22]. Hou *et al.* [23] presented an overview of recent advances in targeting synthetic fluorescent pH probes to some subcellular organelles. However, many of the above-listed fluorescent probes lack the ability to penetrate the cell membrane. Hence, a variety of methods have been proposed for introducing these compounds, including microinjection, hypertonic lysis, scrape loading, and some others [21]. These manipulations can perturb the cell physiology and, in the long run, can have a significant effect on the pH [24].

The green fluorescent protein from *Aequorea victoria* (avGFP) and its homologous fluorescent proteins (FPs) are now the most commonly used probes to visualize the

spatiotemporal dynamics of cells [25, 26]. These fluorophores are genetically encoded, and consequently, no loading procedure is necessary, which ensures noninvasive imaging. Additionally, FPs enable selective targeting to certain cell types, to specific intra/extracellular locations or subcellular compartments by fusing to specific targeting signals. Moreover, FPs have been designed for simultaneous imaging of multiple biochemical events (multiparameter imaging) in a single living cell [27], which is difficult with conventional dyes.

The chromophore of a fluorescent protein is sensitive to subtle changes in its environment [28]. Although wild-type GFP and some FPs are relatively insensitive to changes in ambient pH [29], most of their mutants respond reversibly and quantitatively to pH variations, which is reflected in their absorbance and fluorescence changes. Thus, many FP variants are currently used as versatile tools for monitoring pH in living, unperturbed cells in a time-resolved and organelle-specific manner. The photophysical properties of the avGFP variants used for the development of pH indicators have been reviewed in detail by Bizzarri *et al.* [30]. More recently, Benčina presented an extended list of pH-sensitive FPs and provided an overview of their spectral properties and examples of their applications [31]. Martiniere *et al.* [32] reviewed the new trends in the development of genetically encoded pH sensors optimized for plant cells and tissues.

In this review, we attempt to provide a summary of the progress that has been made during the past two decades in the field of genetically encoded fluorescent pH indicators, with an emphasis on the advantages/disadvantages of each specified method. First, we will consider the current state of the design and applications of FP-based pH indicators, single FP, dual FP, redshifted FPs and FRET-based indicators. We will then turn our attention to the development and applications of hybrid pH sensors that combine the capabilities of non-GFP fluorophores with the advantages of genetically encoded tags. Then, we will discuss the recent advances in multicolor pH imaging, applications of genetically encoded pH sensors in multiparameter imaging and some other modern developments related to the topic.

2. Chromophore protonation states and optical properties of GFP-like proteins

In all wild-type (wt) FPs, the chromophore is formed via consecutive cyclization, dehydration and oxidation autocatalytic reactions within a chromogenic X-Tyr-Gly amino acid sequence [33-36]. These reactions create a GFP-like chromophore, 4-(p-hydroxybenzylidene)-5-imidazolinone (p-HBI), the common core structure of all known FPs of the GFP family (Fig. 1). In FPs with redshifted spectra, p-HBI is the object of additional posttranslational autocatalytic or photoinduced modifications, which extend the π-electron conjugation of the

chromophore (Fig. 1) [37-46]. Basically, the p-HBI chromophore contains two titratable chemical groups, the phenolic hydroxyl group and the imidazolinone nitrogen at the opposite end of the chromophore. However, only two forms, the neutral protonated phenol and the anionic phenolate are considered internally relevant in intact proteins, while the unprotonated state of the imidazolinone ring nitrogen is supposed to be unchanged (Fig. 2A) [47].

In its ground state, wt GFP shows two absorption peaks, the major peak at 395 nm and the minor one at 475 nm (Fig. 2B). It was shown that the 395 and 475 nm peaks represent the neutral phenol and the anionic phenolate of the p-HBI chromophore, respectively [47-49]. However, when excited, both the neutral and anionic species exhibit an emission peak at 508 nm. This unusual phenomenon is associated with excited state proton transfer (ESPT), which upon excitation, enables proton relocation from the chromophore phenol hydroxyl to the carboxylate group of the nearby glutamate 222 via the internal hydrogen bond network (Fig. 2C) [50, 51]. Substitutions of the surrounding amino acids may influence the equilibrium between the neutral and anionic species. Variants with the ground-state equilibrium shifted toward the anionic form are known as enhanced GFP (EGFP) with a fluorescence 35 times brighter than that of wt GFP [52]. By contrast, substitutions that shift the protonation equilibrium to the neutral form and completely block ESPT were used in the engineering of blue-emitting variants of FPs [53].

At physiological pH values, the chromophores of wt GFP and most of wt FPs from Anthozoa are protected from the ambient solvent by the protein shell and begin to titrate only after protein unfolding [48, 54]. In contrast to wt GFP, most naturally occurring FPs from Anthozoa predominantly contain an anionic form of the chromophore. However, unlike wt FPs, most mutant proteins reversibly and rapidly respond to pH variations, changing their absorbance and emission spectra [47]. The chromophore pKa can be tuned by mutagenesis over a broad range from 6 to 8, enabling pH measurements from pH 5 to pH 9. The introduction of amino acids near the chromophore phenolate with proton donor or proton acceptor side chain terminal groups may modulate the chromophore pKa.

3. FP-based pH indicators

Principally, FP-based pH indicators can be divided into two groups, nonratiometric, intensity-based indicators and ratiometric indicators. The first group includes single-peak, intensity-based indicators, which change intensity at a given excitation or emission wavelength in response to pH variations (Fig. 3A). The second group of ratiometric indicators can be subdivided into dual excitation and dual emission pH indicators (Fig. 3B). pH measurement

with these indicators is accomplished by using two excitation lasers (for dual excitation indicators) or by using two detection ranges (for dual emission indicators) when the indicator is excited at one wavelength. The intensity ratios corresponding to excitation at two different wavelengths or the ratio of emission intensities at two wavelengths with excitation at one wavelength are measured, and these data are correlated with the pH by *ex vivo* calibration. Furthermore, ratiometric indicators may be constructed from a single FP with pH-dependent dual excitation or emission properties or from a fusion of two proteins, one of which is a nonratiometric intensity-based pH-sensitive FP and the other one is a pH-insensitive protein used as a reference. Nonratiometric pH indicators are generally used to determine changes in pH and are not suitable for measuring absolute pH values. Ratiometric indicators eliminate measurement distortions induced by FP bleaching, variations in probe concentrations, cell thickness, excitation intensity, detection efficiency, etc. Therefore, using ratiometric indicators allow precise pH measurements and avoid many of the problems related to pH monitoring with nonratiometric sensors.

3.1. Nonratiometric GFP-based pH indicators

Sensitivity to pH variations prompted Kneen et al. to assess the applicability of GFP mutants as targetable, noninvasive indicators of intracellular pH [55]. It was found that upon pH titration, GFP mutants underwent more than 10-fold reversible changes in absorbance and fluorescence and that this response occurred in less than 1 ms. It was also shown that the pKa of the protein could be modulated by different point mutations. The authors obtained GFP mutants with pKa values ranging from 6.0 (for EGFP, GFP-F64L/S65T), 5.9 (S65T) and 6.1 (Y66H) to 4.8 (for T203I). The GFP-S65T mutant demonstrated two absorption maxima at 390 and 490 nm (Table 1). However, in contrast to the wild-type protein, GFP-S65T showed only one excitation maximum at 490 nm with emission at > 510 nm. The intensity of the excitation/emission peaks at 490/510 nm decreased upon a pH change from 8.0 to 5.0. The observed pH-dependent changes in fluorescence occurred in parallel with absorbance changes, suggesting that the molar absorbance rather than the quantum yield of GFP-S65T was affected by the pH changes. To evaluate the capabilities of GFP-F64L/S65T as an intracellular pH indicator, CHO and LLC-PK1 cells were transfected with cDNAs that targeted the mutant to the cytoplasm, mitochondria, Golgi, and endoplasmic reticulum. Fluorescence micrographs showed bright and specific staining of the targeted cellular compartments [55].

Llopis et al. [56] expanded the pKa measuring interval to 6.4 (ECFP, K26R/F64L/S65T/Y66W/N146I/M153T/V163A/N164H/H231L) and to a near physiological value of 7.1 by additional mutations of EGFP (EYFP, S65G/S72A/T203Y/H231L). These

GFPs were targeted to the cytosol plus the nucleus, the medial/trans-Golgi by fusion with galactosyltransferase, and the mitochondrial matrix by using the targeting signal from subunit IV of cytochrome c oxidase. Transfection of HeLa cells and rat neonatal cardiomyocytes with these cDNAs resulted in the expected subcellular localization, as indicated by light and electron microscopy, and reported a local pH that was calibrated *in situ* with ionophores. It was shown that ratiometric measurement of pH is possible by simultaneously cotransfecting cells with pH-sensitive and pH-insensitive (as a reference) proteins [56].

Later, Miesenbock et al. [57] constructed a pH-sensitive mutant of GFP named ecliptic pHluorin (Table 1) and harnessed this protein to monitor pH changes inside secretory vesicles during vesicle exocytosis and recycling. Ecliptic pHluorin carries the substitutions S147D, N149Q, T161I, S202F, Q204T, and A206T, and when pH values are decreasing, this protein gradually loses fluorescence until the complete loss of excitation at 475 nm at pH 6.0. Therefore, at pH values lower than 6.0, the protein is invisible (eclipsed) when excited at 475 nm but can still be weakly seen at 395 nm. pHluorin was fused to the vesicle protein VAMP2, which attached pHluorin to the inner vesicle surface. In the resting state, the interior of vesicles is acidified to a pH of ~5.7, and pHluorin is invisible, remaining in a fluorescence "off" state. After exocytosis, the vesicle interior is exposed to the extracellular medium (pH ~ 7.4), and the pHluorin fluorescence is switched to the "on" state, thereby reporting synaptic neurotransmitter secretion. By introducing two additional mutations (F64L and S65T) into ecliptic pHluorin, Sankaranarayanan et al. created superecliptic pHluorin with higher brightness [58]. Superecliptic pHluorin is almost nonfluorescent at pH 5.5, the pH of intracellular secretory vesicles, but becomes brightly fluorescent when exposed to the extracellular space (pH 7.4). When fused to the appropriate membrane protein, superecliptic pHluorin has been employed to monitor the exocytosis of synaptic vesicles, secretory vesicles, and recycling endosomes. These experiments have led to a number of discoveries [58-63]. Until recently, there was a controversy whether the dopamine D_2 receptor (DRD2) is recycled back to the plasma membrane or targeted for degradation after the dopamine (DA) stimulation. Li et al. [62] used superecliptic pHluorin tagged to N terminus of DRD2 and total internal reflection fluorescent microscopy (TIRFM) to directly examine molecular mechanisms regulating DRD2 insertion to the plasma membrane in cultured mouse striatal medium spiny neurons. Two functionally distinct recycling pathways for DRD2 were discovered: a Rab4-sensitive constitutive recycling pathway that determines steady-state surface expression of DRD2 and a Rab11-sensitive DA activity-dependent recycling pathway that is important for functional resensitization of DRD2.

Compared to the wild-type protein, a GFP mutant (T203Y/S65G/V68L/S72A, YFP) [64] and its related variant constructed from enhanced GFP (EYFP) [56] demonstrate a redshifted

fluorescence spectra due to π-stacking interactions between the chromophore and the Tyr 203 phenol [64]. Both variants show similar pH-dependent fluorescence properties with pKa value of 6.9–7.1. The pKa value of the YFP variant H148G was shown to be 8.0, which may be useful in experiments with organelles such as mitochondria that have elevated pH values. Upon acidification, EYFP shows excitation (514 nm) and emission (527 nm) peaks that decrease with a concomitant increase in the nonfluorescent species that absorbs at 390 nm [56].

Abad et al. [65] used the Ca^{2+} indicator camgaroo-2, which is derived from EYFP [66], in the development of a probe suitable for pH measurements within the mitochondrial matrix. To this end, the Ca^{2+}-sensitive part of camgaroo-2 (calmodulin) was replaced with a portion of aequorin. The obtained pH sensor, termed mtAlpHi, showed an apparent pKa close to 8.5, and the sensor was selectively targeted to the mitochondrial matrix. The fluorescence intensity of mtAlpHi increased (excitation 498 nm, emission 522 nm) with the pH increase from 7.0 to 10.5. Unfortunately, mtAlpHi suffers from a number of drawbacks that are typical for nonratiometric sensors. Quantitative measurements with a single mtAlpHi sensor are the source of potential malfunctions, and it is difficult to interpret the data correctly. To overcome this shortcoming, mtAlpHi was cotransfected with mtECFP because both FPs can be imaged simultaneously and because ECFP is insensitive to pH variations.

On the other hand, the use of YFPs as reporters of intracellular pH is hampered by the fact that the fluorescence intensity of the protein is also dependent on the concentration of halide or nitrate ions [67]. To circumvent this drawback, several mutants of YFPs with reduced chloride sensitivity have been engineered. However, the halide-resistant mutant termed Citrine showed a substantially reduced pKa value of 5.7, limiting the scope of applications to the more acidic species such as secretory and endocytic organelles [66].

3.2. Ratiometric single-protein GFP-based pH indicators

In addition to the dependence on the pH of the surrounding medium, the fluorescence intensity of FPs also depends on some other variables, such as the expression level of the gene and photobleaching. Therefore, the absolute pH value cannot be determined from only changes in the fluorescence intensity. To overcome these ambiguities, researchers constructed ratiometric pH indicators with pH-dependent dual excitation or dual emission properties. By calculating the intensities ratio at two wavelengths, it is possible to quantify absolute pH values.

Along with ecliptic pHluorin, Miesenbock et al. [57] developed ratiometric pHluorin (Table 2). For conversion to a ratiometric pH sensor, the substitutions S202H, E132D, S147E, N149L, N164I, K166Q, I167V, R168H and L220F were introduced into wt GFP. The

excitation peak intensity of ratiometric pHluorin at 395 nm increased, and the excitation intensity at 475 nm decreased upon a pH change from 5.5 to 7.5, with a response time of < 20 ms [57]. Later, an enhanced ratiometric pHluorin (pHluorin2) was developed by introducing the additional F64L mutation to GFP containing fully mammalianized codons and ten of the thirteen pHluorin-specific mutations. The resulting pHluorin2 displayed markedly higher florescence than pHluorin while maintaining the ratiometric pH sensitivity [68].

However, even with ratiometric sensors, some imaging artifacts must be taken into account. For example, cell autofluorescence contributes differentially to the pHluorin signal at different wavelengths. Appropriate corrections should be made by measuring the autofluorescence in control samples of pHluorin-untransformed cells; this autofluorescence is subtracted from the aggregate fluorescence of cells transformed with the pH sensor. In another approach, correction for the autofluorescence was significantly simplified and the sensitivity of pH assays was increased by taking advantage of the synchronously scanned florescence spectra of pHluorin in cell suspensions [69].

Serresi et al. [70] used a GFP variant F64L/T203Y, termed E^1GFP, as a ratiometric pH indicator with a pKa of ~ 6.0. E^1GFP was shown to be virtually insensitive to halide ions, and consequently, E^1GFP may be used for pH measurements in subcellular compartments where the pH decrease is accompanied by an increase in the chloride ion concentration. By fusing E^1GFP to the HIV-Tat protein, which endows the pH reporter with cell-penetrating properties, the authors were able to monitor the whole process of cellular endocytosis in real time from the initial cell-surface binding to the multistep endocytic pathway. After cellular internalization, Tat-E^1GFP exhibited two distinct intracellular species: the first was observed close to the plasma membrane, and the second was embedded in the cytoplasm. After 4 h of incubation, vesicles associated with the membrane showed an almost neutral pH of 6.77, whereas after two more hours of incubation, the pH dropped to the mean value of 6.31 [70]. However, the low pKa of E^1GFP permits pH measurements only within specific intracellular regions that impose limitations on the use of this probe. By introducing F64L/S65T/T203Y substitutions, the same group constructed a ratiometric pH sensor named E^2GFP [71]. E^2GFP showed changes in both excitation and emission fluorescence spectra upon pH variations (Table 2). With a pKa close to 7.0, E^2GFP was used to determine the average intracellular pH (pHi) and spatial pHi maps in different cell lines under physiological conditions.

Based on GFP, Hanson et al. [72] constructed several ratiometric dual emission pH-sensitive variants, termed deGPFs. deGFPs display pKa values ranging from 6.8 to 8.0 and show variable emission wavelengths shifting between the green (λmax ~ 515 nm) and blue forms (λmax ~ 460 nm) upon the pH decrease. For the deGFP1 variant (S65T/H148G/T203C,

pKa ~ 8.0) and the deGFP4 variant (S65T/C48S/H148C/T203C, pKa ~ 7.3), the underlying conditions for variable emission were analyzed in the most detail (Table 2). Crystal structure analyses of deGFP1 suggest that the basis for dual emission is the distortion of the wild-type proton-transfer network by the S65T substitution. It was suggested that at low pH, the modified protein structure lacks a hydrogen bond network that in the excited state supports rapid proton transfer from the neutral chromophore to an acceptor. Therefore, at low pH, ESPT is interrupted, and the fluorescence from the neutral chromophore appears blue. At high pH, backbone rearrangements restore the hydrogen bond network that enable the ESPT from the excited state of the neutral chromophore to the bulk solvent, resulting in green emission from the anionic chromophore [72]. The applicability of deGFP4 as a pH sensor in mammalian cells was tested by transient expression of this variant in PS120 fibroblasts. In contrast to conventional confocal microscopy, which showed cytoplasmic fluorescence only marginally above the cellular autofluorescence in the blue channel (385-475 nm), a superior above-background signal was obtained by two-photon excitation microscopy [72].

Schmitt et al. [73] suggested an alternative technique to differentiate the deGFP signal from the undesirable autofluorescence background. As the fluorescence lifetime is an inherent characteristic of deGFP, it is possible to quantify the contribution of the background from a single decay curve at a fixed wavelength. The authors performed quantitative analysis of pH in cells using fluorescence lifetime imaging microscopy (FLIM) with superior precision. deGFP4 (termed eGFP-pHsens) was either expressed in the cytoplasm or targeted to the mitochondria of CHO-K1 cells and was exploited as a pH sensor to monitor activity of the M2 proton channel from influenza A virus. After excitation of eGFP-pHsens at 405 nm, the simultaneous ratiometric (460 nm vs. 520 nm) and kinetic analysis (at 520 nm) of its fluorescence properties was accomplished [73].

In another approach, Battisti et al. [74] used phasor-based FLIM. Phasor analysis of FLIM-based pH measurements using E^2GFP as a pH indicator allowed fast graphical determination of pH maps and required only a preliminary phasor calibration. This technique proved to be effective in discriminating the autofluorescence signal from the E^2GFP emission, as the autofluorescence phasors clearly fell outside the segment accounting for all pH values measured by the indicator.

Much attention has been paid to the physiological impact of intracellular pH and pHi regulation in recent years [75]. Unfortunately, the physiological relevance of extracellular pH alterations has been studied to a much lesser extent. It was shown that extracellular acidification occurs in the brain with the elevated neural activity and neuronal injury [76]. Chiacchiaretta et al. [77] studied the spatiotemporal dynamics of extracellular pH changes

during epileptic-like neuronal hyperexcitability in primary neuronal networks. To quantify variations in extracellular pH, E^2GFP, a ratiometric GFP-derived pH sensor [71], was fused to the N-terminus of the PDGF receptor transmembrane domain, exposing the sensor to the extracellular side of the plasma membrane (ex.E^2GFP). Unlike the situation for pHluorin, whose fluorescence quenches upon acidic pH shifts, the emission intensity of E^2GFP excited at 405 nm increases as the pH drops, enabling possible more sensitive and quantitative measurements of extracellular acidification. Monitoring ex.E^2GFP fluorescence in primary cortical neurons allowed quantification of the pH fluctuations during network hyperexcitability induced by convulsant drugs or high frequency electrical stimulation. It was found that neuronal hyperactivity causes acidic shifts localized to active synapses and generated by Na^+/H^+ exchanger activity [77].

On the basis of HyPer, a H_2O_2 indicator derived from a circularly permuted yellow fluorescent protein [78], Poburko et al. [79] created a ratiometric pH indicator. Substitution of the H_2O_2-sensing cysteine residue 199 with a serine caused a complete loss of HyPer sensitivity to H_2O_2, leaving the sensitivity to hydrogen ions unchanged. The combination of a mitochondrially targeted HyPer with the cytosolic pH indicator SNARF allowed concurrent estimates of pH in the cytosol and mitochondrial matrix and consequently permitted real-time measurement of the intact cell cytosol-matrix pH gradient. Matlashov et al. used an improved version of HyPer, termed HyPer-2, with an A406V substitution [80]. Introduction of the mutation C199S into HyPer-2 resulted in an improved version of the pH sensor, named SypHer-2. SypHer-2 showed two excitation peaks (at 420 nm and 500 nm) and one emission peak at 516 nm, similar to HyPer. However, in contrast to SypHer, SypHer-2 had a 2- to 3-fold brighter fluorescence signal in mammalian cells. SypHer-2 was used for monitoring pH changes both *in vitro* and *in vivo* [80] and for pH_i mapping in living cancer cells [81]. Recently, an improved version, termed SypHer3s (Table 2), was engineered by random mutagenesis of HyPer C199S and by screening the mutants in *E. coli* libraries for enhanced brightness [82]. The SypHer3s gene contains three mutations: Y145F, D129G and Q197L. It was proposed that the Y145F substitution is the key condition for the increased brightness. SypHer3s exhibits two excitation maxima at 410 nm and 495 nm and a single emission maximum at 525 nm. When the pH increases, the intensity of the 410 nm band decreases, with an intensity increase for the 495 nm band. SypHer3s was used for real-time pH imaging in the mitochondria of living neurons and for ratiometric pH measurements in zebrafish embryos [82].

3.3. Redshifted FP-based pH indicators and multicolor pH imaging

To overcome the cellular autofluorescence problem, many GFP mutants have been engineered; these mutants include variants with redshifted emission, like the yellow fluorescent protein. However, many of these variants suffered from low brightness and high sensitivity to different environmental conditions [67, 83]. It was the discovery of redshifted GFP homologs from Anthozoa species that provided new opportunities for the development of novel fluorescent tools [84]. The red emission circumvented the problem associated with the background autofluorescence, since the autofluorescence in most eukaryotic cells is reduced at longer wavelengths. Moreover, the redshifted fluorescence permitted deep-tissue and whole-body experiments because longer wavelengths penetrate cellular tissues much more effectively than shorter wavelengths. In addition, multicolor imaging with different FP spectral variants added a new dimension to the fluorescent toolbox, as simultaneous measurements of different cellular parameters became feasible. For example, labeling with a red FP-based pH indicator in combination with green or yellow pH sensors allowed simultaneous pH measurements in different cellular compartments [85].

However, the obligate tetramerization of FPs from reef corals and anemones [29] was another problem that hampered the development of redshifted biosensors. In particular, it was a general problem when an FP was fused to a host protein that was targeted to a specific subcellular location. Oligomerization of FPs often produced improper localization and sometimes caused cytotoxic effects. Subsequently, a number of monomeric redshifted variants suitable for biosensor development have been engineered [86-88]. Some monomeric variants from the so-called mFruits series [87], which were derived from the red FP cloned from *Discosoma* sp. [84], showed a relatively high sensitivity to pH changes [89, 90].

mNectarine (Table 3), an optimized version of mTangerine (the Q66C/T147S/Q213L variant of mRFP1), proved to be suitable for measuring physiological pH changes in mammalian cells [90]. mNectarine showed an apparent pKa of 6.9, a fluorescence excitation peak at 558 nm and an emission peak at 578 nm. Both purified mNectarine and mNect-transfected HEK 293 cells demonstrated decreased fluorescence with decreasing pH. mNectarine was fused to the cytosolic N-terminus of human nucleoside transport protein (hCNT3) to generate mNect.hCNT3. The chimeric protein mNect.hCNT3 enabled pH measurements at the intracellular surface of hCNT3, providing insight into the mechanism of hCNT3 H+/uridine cotransport.

Another intensiometric redshifted sensor, pHTomato (Table 3), was developed by Li and Tsien [91] by DNA shuffling and semirandom mutagenesis starting with mRFP and mStrawberry [86, 87]. pHTomato, which is derived from mStrawberry, differs from

mStrawberry by six amino acid substitutions (F41T, F83L, S182K, I194K, V195T and G196D). pHTomato shows an excitation wavelength at 550 nm and emission maximum at 580 nm with a pKa close to 7.8. Although the emission intensity of pHTomato demonstrates considerable pH dependence, with higher fluorescence intensity as the pH increases, its excitation and emission wavelengths are pH independent. pHTomato can be used in parallel with green-emitting probes to detect neuronal activity. The fusion of pHTomato to the vesicular membrane protein synaptophysin (sypHTomato) allowed monitoring activity-dependent exocytosis as efficiently as with green-emitting reporters. The redshifted emission of pHTomato was harnessed in multicolor imaging experiments (Fig. 4). Coexpression of sypHTomato with the GFP-based Ca^{2+} indicator GCaMP3 in the same neuron enabled concomitant imaging of transmitter release and presynaptic Ca^{2+} transients at single nerve terminals. When expressing sypHTomato and GCaMP3 in separate cells, it was possible to simultaneously monitor presynaptic vesicular turnover and postsynaptic sub- and suprathreshold responses from a connected pair of neurons [91].

Shaner et al. [92], by random and iterative mutagenesis, engineered two highly photostable wavelength-shifted mRFP derivatives, mOrange (excitation maximum at 548 nm, emission maximum at 562 nm) and mOrange2 (excitation maximum at 549 nm, emission maximum at 565 nm), with a pKa of 7.5 and 6.5, respectively. mOrange and mOrange2 (Table 3) show enhanced photostability, efficient maturation, and increased pH sensitivity [92, 93], but display undesirable photoswitching behavior, hampering the pH imaging [94]. Similar to the situation for pHluorin, the fluorescence of mOrange2 is quenched by lowering the pH below 5.5 and is restored at neutral pH values. This property of mOrange2 was used to image synaptic vesicle recycling [93]. mOrange2 was fused to the vesicular glutamate transporter VGLUT1. To improve the signal-to-noise ratio, two molecules of mOrange2 in tandem were inserted into the same intraluminal loop of VGLUT1 to create the VGLUT1-2XmOr2 pH sensor. To follow the changes in calcium concentration, the synaptic vesicle protein synaptophysin was fused to the GFP-derived calcium indicator GCaMP3. Dual color imaging of changes in the green and red fluorescence of neurons coexpressing the two reporters enabled monitoring the time course of changes in VGLUT1 recycling in relation to changes in the presynaptic calcium concentration [93].

Unlike superecliptic pHluorin, the redshifted pH sensors pHTomato and mNectarine demonstrate a significantly reduced pH sensitivity. Compared to the more than fifty-fold fluorescence change in superecliptic pHluorin upon transitions between pH 5.5 and 7.5, mNectarine and pHTomato show only six- and three-fold changes, respectively, over the same pH range. To overcome these limitations, Shen et al. invested substantial efforts in the

development of a redshifted pH sensor with a dynamic range comparable to that of superecliptic pHluorin [95]. Starting from mOrange, four bright variants, named pHorans, were constructed by site-directed mutagenesis and several rounds of random mutagenesis. This series of orange pH sensors showed pKa values ranging from 6.7 to 7.5. The fluorescence fold change of these variants varied from 10 to 17 when the pH changed from 5.5 to 7.5. Furthermore, the red fluorescent pH sensor pHuji, with an emission peak well separated from that of superecliptic pHluorin, was constructed with mApple as a template [95]. pHuji (Table 3) demonstrates a more than 20-fold fluorescence intensity change in response to a pH shift from 5.5 to 7.5 and outperforms the reported intensity change of other redshifted pH sensors. pHuji was used in conjunction with superecliptic pHluorin for simultaneous imaging of exocytic and endocytic events. Dual color imaging of the clathrin-mediated internalization of the transferrin receptor and the β2 adrenergic receptor revealed differential sorting of the two receptors at the time of endocytic vesicle formation.

In contrast to the intensiometric pHorans and pHuji, pHRed (Table 3) represents the first ratiometric, single-protein red fluorescent sensor of pH [96]. pHRed (pKa ~ 6.6) was engineered from the long Stokes shift red fluorescent protein mKeima by the A213S substitution. pHRed exhibits a fluorescence emission maximum at 610 nm and dual excitation peaks at 440 and 585 nm that can be used for ratiometric imaging. A pH decrease from 9 to 6 causes a 7-fold increase in the 585 nm peak intensity and a 4-fold decrease in the 440 nm peak intensity. Notably, the ratio response of pHRed is insensitive to the buffer ion components, including alkali metals, chloride ions, and oxidative agents, and to temperature (21-37°C). pHRed was targeted to the mitochondrial matrix and used to probe mitochondrial function. Moreover, pHRed was used in multicolor experiments in combination with a circularly permuted mVenus-based ATP/ADP sensor [97] to simultaneously image intracellular ATP and pH and to monitor energy-dependent changes in cytosolic pH [96].

3.4. Ratiometric dual-FP-based pH indicators

Another approach in the development of pH sensors is based on two tandemly linked fluorescent proteins with well-separated fluorescence maxima. One of these proteins is pH sensitive and represents the pH-indicating part of the fusion; the other one is pH insensitive and serves as a reference (Fig. 3C). These dual-protein pH indicators provide a valuable addition to the toolbox of ratiometric pH sensors. In addition, the utilization of varying combinations of FPs provides a wide range of choices appropriate for every specific biological system.

In 2001, Awaij et al. [98] were the first to construct ratiometric pH sensors (termed GFpH and YFpH) composed of the tandemly linked pH-insensitive GFPuv variant and pH-

sensitive GFP (EGFP or EYFP) derivatives (Table 4). GFpH represents the fusion of GFPuv and EGFP and has two excitation maxima at 380 nm and 480 nm, which correspond to GFPuv and EGFP, respectively. The intensity of both excitation peaks (*F*) decreased upon lowering the pH, and the ratio *F*480/*F*380 as a function of pH was approximately fitted by a sigmoid curve at pH 5.5–7.5 with an apparent pKa of 6.2. GFpH proved to be suitable for monitoring pH changes in the range between 6.0 and 7.5; GFpH is characterized by poor sensitivity to changes in Cl^- concentration [98]. Another probe, YFpH, consists of the fusion between GFPuv and EYFP. YFpH was shown to have substantial sensitivity to Cl^- concentration changes due to the presence of EYFP. It was also shown that YFpH can be considered a FRET-based indicator, which will be discussed in the next section.

Rosado et al. [99] developed a dual color‐emission biosensor, Rosella (Table 4), the fusion of a pH‐insensitive fast‐maturing red fluorescent protein variant, DsRed.T3, with the pH‐sensitive superecliptic pHluorin. The fluorescence emission of DsRed.T3 is stable over the pH range of 4.9‐9, and the fluorescence emission of superecliptic pHluorin (λmax emission 508 nm) is quenched below pH 6.2. The operation of the sensor relies on the pH difference between the vacuole (or lysosome, pH 6.2 or 4.8, respectively) and the other cellular compartments (usually pH > 7.0). Rosella was harnessed to monitor the vacuolar turnover of the cytosol and organelles. The probe was expressed in the cytosol and targeted to mitochondria or to the nucleus in yeast (*Saccharomyces cerevisiae*). It was demonstrated that Rosella can be used as a reporter of autophagy by employing fluorescence-activated cell sorting of discrete populations of cells undergoing autophagy [99]. However, Rosella requires a dual excitation and dual emission procedure, which complicates experiments that require imaging of rapid events in highly motile structures.

In contrast to other types of endocytosis, macropinocytosis is susceptible to inhibitors of Na+/H+ exchange (NHE). However, the relationship between NHE and macropinosome formation currently remains unclear. One possible mechanism is that the effect of NHE on macropinocytosis may be mediated by changes in cytosolic pH. To explore the factors that are responsible for macropinocytosis, Koivusalo et al. [100] used different pH-sensitive compounds to evaluate the effect of pH changes. The bulk cytosolic pH was measured with the synthetic ratiometric dye seminaphthorhodafluor-5 (SNARF-5F), whereas the pH of the inner part of the plasma membrane was monitored with a genetically encoded ratiometric pH probe, superecliptic pHluorin fused to the pH-insensitive mCherry (Table 4), which was targeted to the inner region of the plasma membrane by inclusion of the N-terminal motif of the Src family kinase Lyn [101]. The superecliptic pHluorin-to-mCherry fluorescence ratio varied almost linearly with pH in the 6.8–7.8 range, in accordance with pKa = 7.2 reported for superecliptic

pHluorin. Using this novel submembranous pH sensor, the accumulation of the metabolically generated acid at sites of macropinocytosis was detected [101].

There is emerging evidence that variations in H^+ concentration may serve as a signaling mechanism in plant cells. The pH control in the cytosol and in the apoblast is important for nutrient and sugar transport across the plasma membrane, as well as for the regulation of cell elongation and organ development. To monitor pH changes in plant cells, a new genetically encoded sensor, pHusion (Table 4), was designed [102]. pHusion is composed of two tandemly fused fluorescent proteins, mRFP1 and EGFP. EGFP (pKa = 6.2) is very sensitive to differences in pH, and mRFP1 is virtually insensitive to pH changes in the physiological pH range, with a pKa of 4.5. The two fluorescent proteins were linked by a short linker, enabling ratiometric measurements of pH changes, where mRFP1 functioned as an intramolecular reference. pHusion was targeted to the cytosol or the apoplast. An apoplastic-targeted version of pHusion was generated by placing a target signal peptide originating from an *Arabidopsis* chitinase in front of mRFP [103]. Rapid pH homeostasis upon external pH changes was reflected by the negligible cytosolic pH fluctuations, while the apoplastic pH changed drastically.

In experiments that require monitoring of the autophagic process, microtubule‐associated protein 1 light chain 3 (LC3) is widely used as a marker protein. Kimura et al. developed mRFP‐GFP tandem‐tagged LC3 to analyze the autophagosome maturation process [104]. mRFP‐GFP-LC3 showed both GFP and mRFP fluorescence signals before the fusion with lysosomes and exhibited only the mRFP signal afterward. Using this reporter, the authors were able to provide evidence that overexpression of a dominant negative form of Rab7 interrupted the fusion of autophagosomes with lysosomes, implying that Rab7 is involved in this step.

In a similar approach, Tresse et al. constructed the mCherry-EGFP-LC3 probe to monitor autophagosome maturation [105]. Both mCherry and EGFP emit fluorescence at neutral pH; therefore, LC3-positive vesicles appear yellow in merged images. Upon vesicle acidification, the fluorescence of EGFP is quenched, and only mCherry emits fluorescence, making LC3-positive vesicles appear red. Thus, the reporter permits monitoring of autophagosome maturation through changes in the fluorescence emission spectra upon vesicle acidification.

To acquire a more detailed picture of the autophagy process, Maulucci et al. [106] used tandemly linked EGFP and mRFP as a dual-emission ratiometric probe to monitor autophagic flux. Due to its compact folding, GFP is relatively resistant to lysosomal proteases. At the low pH values characteristic of the autolysosome, the fluorescence signal of GFP is quenched, whereas the fluorescence of mRFP is not quenched in autolysosomes. The pH dependency of

the fluorescence emission spectra was measured at a single excitation wavelength, 488 nm. By exploiting these differences in fluorescence emission, autophagic flux can be morphologically traced with this pH sensor. This technique allows imaging the number and the pH of autophagy intermediates. According to the analysis, 3 major populations were dissected with a continuous rather than discrete pH distribution of each population in the range of 4.5–6.5 [106]. mRFP-EGFP was targeted to autophagosomes by fusion of a dual protein in tandem with LC3.

Although tandem mRFP/mCherry-EGFP-tagged LC3 (-LC3) provides a convenient means of monitoring autophagic flux, there is still weak EGFP fluorescence in acidic environments between pH 4 and 5, which sometimes leads to misinterpretation of autophagic flux experiments. To construct a pH sensor, Zhou *et al.* [107] used mWasabi FP that was more sensitive to acid than EGFP was. Compared with mRFP-EGFP-LC3, the mTagRFP-mWasabi-LC3 reporter has no fluorescence in acidic lysosomes, shows much brighter fluorescence, and provides more precise and accurate results when monitoring autophagic flux.

As already mentioned above, redshifted biosensors allow deep-tissue and whole-body experiments because longer wavelengths penetrate cellular tissues more effectively. Tanaka et al. [108] used tandemly linked Venus FP (YFP variant) [109] as a pH-sensitive unit and monomeric DsRed as an internal standard. In contrast to YFP, Venus has decreased sensitivity to changes in Cl^- concentrations, and in contrast to GFP-based pH sensors (pKa ~ 6.0), YFP (pKa ~ 7.1) can be used for measurements in alkaline media. In contrast to normal differentiated cells, with an intracellular pH maintained within the narrow range of 6.9–7.1, the hallmark of tumor cells is an elevated intracellular pH (pH 7.2–7.7) [110]. HeLa cells permanently expressing the VenusFP-mDsRed probe were inoculated into a nude mouse, and fluorescence image ratios were used to visually determine the intracellular pH of the tumor xenograft model [108].

3.5. Dual-FP Förster resonance energy transfer (FRET)-based pH indicators

When two FPs form a tandemly fused construct, the fluorophores in the pair are in close proximity to each other. If the emission spectrum of one fluorophore has a strong overlap with the absorption spectrum of the other fluorophore, then FRET may occur [111]. FRET is a light-induced process by which the excited-state energy of a shorter-wavelength fluorophore, or donor fluorophore, is transferred to a longer wavelength fluorophore (acceptor fluorophore) via nonradiative dipole–dipole coupling. For effective FRET, the two most crucial parameters to consider are the quantum yield of the donor and the molar extinction coefficient of the acceptor. When the quantum yield of the donor or the molar extinction coefficient of the acceptor is pH sensitive, the tandemly fused FRET pair may be used as a ratiometric pH-

sensing probe (Fig. 3D). In some cases, FRET-based pH indicators are advantageous, since these probes require only a single excitation wavelength, which simplifies the detection system.

Awaji et al. [98] were the first to develop a tandemly fused FRET-based pH indicator with the abbreviated name YFpH (Table 4). YFpH is composed of GFPuv (donor) and EYFP (acceptor). Upon excitation at 380 nm, YFpH shows two emission components with a maximum at 509 nm in the pH range between 5.0 and 6.0 and with a peak at 527 nm for pH 7.0–8.5, which correspond to the emission maxima of GFPuv and EYFP, respectively. Consequently, EYFP is excited by the emission of GFPuv via FRET, since EYFP is not excited directly by 380 nm UV light. When excited at 380 nm, the emission maximum of YFpH is shifted from 509 to 527 nm upon a pH increase between pH 6.0 and 7.0. In contrast, the emission intensity of YFpH at 520 nm upon 380-nm excitation remained almost unaltered in the pH interval of 6.0–8.5, implying that the rate of FRET-mediated fluorescence is increased when the pH is raised. Therefore, YFpH may be used not only as a dual excitation pH indicator but also as a dual emission pH sensor. YFpH was expressed in the cell lines COS-7 and CHO-K1, and fluorescence was detected by confocal microscopy in the cytoplasm and nucleus. The pH-dependent alteration in the fluorescence intensity ratio (dual-excitation mode) of the expressed YFpH was measured after the cells were made H^+-permeable by the addition of the H+ ionophores nigericin and monensin to the medium [98].

Cyan (CFP) and yellow (YFP) FPs are the most often used pair for FRET-based imaging studies because these FPs share a significant spectral overlap. CFP is a GFP mutant with a Y66W substitution. With tryptophan in place of the tyrosine residue, the chromophore of CFP lacks a titratable phenolic group, and the fluorescence spectra of CFP are poorly sensitive to pH variations. Therefore, CFP can be used as the pH-insensitive part of the fusion and YFP as the pH-sensing unit. When the pH is lowered, the extinction coefficient of YFP decreases. This decrease reduces the spectral overlap between the donor and the acceptor and leads to a donor emission increase and to a decrease in the acceptor emission. By calculating the ratio of the donor-to-acceptor fluorescence intensities, it is possible to acquire a quantitative pH readout.

Using YFP variants in a fusion with ECFP, Esposito et al. designed a FRET-based pH sensor platform covering the pKa values within the range of 5–7 [112]. This new family of pH biosensors, called pHlameleon (Table 4), includes three ratiometric sensors. The first sensor takes advantage of a previously developed highly efficient FRET pair consisting of the concatenated variants of ECFP and YFP Venus (named Cy11.5) [113]. In the second sensor, the truncated Venus is replaced with a similarly truncated EYFP, and the third sensor contains the EYFP-H148G mutant as an acceptor fluorophore [112]. The first pH sensor, termed

pHlameleon 5 according to its pKa value (Table 4), can be used as a very sensitive ratiometric pH biosensor at low pH values, for instance, to image intralysosomal changes. EYFP and EYFP-H148G both exhibit higher pKa values (6.9 and 7.9, respectively) than that of Venus. The ECFP-EYFP fusion construct, called pHlameleon 6, exhibits the pKa of 6.2 and is sensitive within the pH range of 5.0–7.5, which is highly physiologically relevant. To extend the pH-sensing range, the H148G mutation was introduced into pHlameleon 6. This change resulted in the expected shift of the pKa to 7.1 but also caused a further loss of energy transfer.

In addition to ECFP, several improved cyan fluorescent proteins such as mCerulean3 [114], mTurquoise2 [115], and Aquamarine [116] were recently developed. These proteins exhibit a higher fluorescence quantum yield, high photostability, longer mono-exponential lifetime and faster maturation. These new CFPs are spectrally identical to ECFP and can therefore be used as a substitute for ECFP in FRET constructs [117]. To further reduce the pH sensitivity of the donor, Betolngar et al. [118] replaced ECFP with Aquamarine in a CFP-YFP tandem fusion and quantified the pH-dependent FRET efficiencies in cyan-yellow FRET pairs and in a biosensor of cAMP-dependent kinase activity. Combining live cell fluorescence lifetime imaging microscopy and the well-known methods of manipulation of the intracellular pH, the authors revealed the complex impact of pH on the FLIM and ratiometric signals of FRET biosensors carrying CFPs and YFPs in living cells.

4. Hybrid pH sensors

Up to this section, the discussion concerned only pH sensors composed of GFP-like proteins. However, these probes share several drawbacks, such as the comparatively low photostability and the extended protein folding and chromophore formation phases, which result in a time lag in the observed fluorescence signal of the reporter. Tandemly fused FPs quite often show different maturation or chromophore formation times [119] and exhibit differential photobleaching over time, which may preclude their use for extended pH imaging. Moreover, redshifted FP-based pH sensors are markedly inferior to superecliptic pHluorin with their significantly reduced pH sensitivity, low brightness and nonoptimal pKa values. To circumvent these limitations, hybrid sensors were developed [120] that combined the capabilities of non-GFP fluorophores with the advantages of genetically encoded tags.

To overcome the problems of redshifted FP-based pH sensors, Martineau *et al.* [121] developed "semisynthetic" pH-sensitive protein conjugates with organic redshifted fluorophores, carbofluorescein (CFl) [122] and Virginia Orange (VO) [123], which show pH sensitivities similar to that of superecliptic pHluorin (Fig. 5A). Compared with fluorescein, CFl and VO are redshifted with λex/λem = 544 nm/567 nm and 555 nm/581 nm, respectively. CFl

and VO display pKa values of 7.5 and 6.7 and a Hill coefficient of 1.6 and 1.5, respectively. CFl exhibits a photobleaching rate similar to that of fluorescein, whereas VO is two to three times more photostable. These fluorophores were used as probes for exo- and endocytosis in two ways. First, benzylguanine derivatives of fluorophores were synthesized and specifically attached to the genetically encoded self-labeling SNAP tag [124] (Table 5). In the second way, a monoclonal antibody targeted to the extracellular epitope of a vesicular protein, synaptotagmin 1, was labeled with VO, which allowed imaging of synaptic vesicle fusion events in living cells [121].

In another approach, Dennis et al. [125] constructed a ratiometric pH sensor comprising a bright and photostable semiconductor quantum dot (QD) as a FRET donor and fluorescent proteins, mOrange or its variant mOrange M163K, as pH-sensitive acceptors (Table 5). QDs are known to be excellent FRET donors due to their exceptional brightness, high quantum yields, photostability, capacity to bind multiple acceptor molecules, and narrow and tunable emission spectra [126]. The constructed FRET pairs composed of GFP-like FPs and QDs exhibit high energy transfer efficiencies, enabling ratiometric measurements with high sensitivity. Due to the pH-dependent molar extinction coefficients of mOrange and mOrange M163K, the excitation and emission spectra of both FPs vary upon pH changes. According to the pKa values of 6.9 and 7.9 for mOrange and mOrange M163K, respectively, these FPs may be considered optimal acceptors for sensitive detection in or near the physiological pH range. Both proteins were conjugated to QDs via standard carbodiimide chemistry, and the absorbance spectra indicated an average of 15.7 and 16.5 proteins conjugated to a single QD for mOrange and mOrange M163K, respectively. To demonstrate the applicability of the QD-mOrange probe for live cell pH imaging, the construct was modified with a polyarginine sequence at the C-terminus for cellular delivery and to facilitate the endosomal uptake of QD-FP [127].

Recently, an alternative family of fluorescent proteins that bind flavin mononucleotide (FMN) as a chromophore has been developed [128]. In contrast to GFP-like proteins, which show a decreased fluorescence signal intensity upon oxygen deficiency, FMN-binding fluorescent proteins (FbFPs) demonstrate bright cyan-green fluorescence under both aerobic and anaerobic conditions. Rupprecht et al. [129] used the FMN-binding fluorescent protein EcFbFP for a donor domain and EYFP variants as acceptors to develop tandemly fused, genetically encoded FRET-based pH biosensors (FluBpH) (Fig. 5B). In contrast to many FPs of the GFP family, EcFbFP exhibits a remarkable tolerance for acidic pH (pKa ~ 3.2). Three EYFP variants with pKa values of 5.7, 6.1 and 7.5 were used in the constructs as pH-sensing domains (Table 5). The corresponding biosensors FluBpH 5.7, FluBpH 6.1 and FluBpH 7.5

were calibrated *in vitro* and *in vivo* to accurately evaluate their pH-sensing properties. The applicability of FluBpH for ratiometric live cell pH measurements was demonstrated by monitoring pH changes in living *E. coli* cells during acidic stress [129].

Many organelles in the endocytic pathway are smaller than 250 nm in size, which is below the diffraction limit of conventional light microscopy. Recent advances in super-resolution fluorescence microscopy (nanoscopy) enabled imaging of cells at a subdiffraction resolution of 50 nm or even better [130]. To monitor the acidification of individual vesicles during endocytosis, cargo sorting and degradation, Richardson et al. [131] developed a family of ratiometric endosomal pH sensors (SRpHi) specifically designed for the use in live cell STED nanoscopy. In this design, fluorescent proteins (EYFP, EGFP, superecliptic pHluorin) with reversible, acid-sensitive fluorescence quenching were fused to the 10 amino acid cell-penetrating Tat-peptide from HIV-1 (GRKKRRQRRR). The TAT-fused fluorescent proteins were further labeled with the Abberior STAR400, STAR410, or STAR512 dyes. The four resulting pH-sensing probes showed pKa values in the interval of 5.9–7.1, which allowed measurements in the pH range of 4.5–7.5. The SRpHi probes enabled subdiffraction live cell imaging of pH changes within endosomes and their associated structures. Importantly, uptake of the SRpHi probes did not appear to affect normal endosomal trafficking or have any other adverse effects on the live cells [131].

The shortcoming inherent to all fluorescent pH sensors is associated with the fluorescence excitation, which is accompanied by photobleaching, the high background of cell/tissue autofluorescence, and the poor penetration of excitation light into tissues. Therefore, pH sensors with no need for excitation light would be advantageous especially for whole-body experiments. To circumvent these limitations, Zhang et al. [132, 133] used bioluminescence resonance energy transfer (BRET) instead of FRET. By fusing a bright mutant of Renilla luciferase, RLuc8 [134], as the donor to a circularly permuted Venus FP [135] acceptor (Fig. 5C), the authors developed a tandem protein, called pHlash (Table 5), that showed a dramatic pH-dependent change in its emission spectrum. When the pH increased, the BRET ratio (the 525 nm/475 nm emission ratio) of the tandem protein also increased. Importantly, neither $CaCl_2$, $MgCl_2$, NaCl, nor KCl had a significant effect on the spectral response of pHlash to pH changes. The applicability of the probe was demonstrated in yeast and HeLa cells [132].

One of the drawbacks of FP-based pH sensors is their ubiquitous labeling of the total population of the expressed target protein. However, upon endocytosis, it is difficult to discriminate newly internalized pH-sensitive FP-tagged receptors from the resident intracellular pool of FP-tagged receptors. In addition, the latter receptors contribute to the background signal from incompletely quenched FPs or previously internalized proteins in

various cellular compartments. To address this issue, Perkins *et al*. [136] engineered a family of excitation ratiometric, cell surface protein-labeling pH sensor complexes (TRApHIC), which consist of a pH-sensitive Cy3 donor bound to a pH-insensitive fluorogenic malachite green acceptor. Upon binding of the complex to a fluorogen-activating protein (FAP) comprising single chain antibodies isolated from a yeast cell surface display library, the otherwise dark fluorogenic malachite green dye is activated and displays a thousand-fold fluorescence enhancement [137, 138]. When bound to the FAP, the complex exhibits dual fluorescence excitation with far-red emission and an excitation ratio dependent on the pH of the medium due to the variable FRET efficiency. The established family of pH-sensitive Cy3 analogues covers a range of pKa values, allowing measurements of extracellular pH changes or changes in the endocytic/recycling pathway. Since genetically encoded FAPs are small, it is possible to fuse FAPs to any protein of interest for live cell imaging. Using FAP-tagged β2-adrenergic receptor (B2AR) and cell membrane-impermeable TRApHIC, quantitative profiling of receptor endocytosis and recycling at the single-vesicle level proved to be feasible, revealing the differences among various B2AR agonists [136].

5. Genetically encoded pH sensors and multiparameter imaging

With the advent of genetically encoded fluorescence reporters, the research community gained a noninvasive toolbox enabling targeting of the probe to certain cell types and specific intra/extracellular locations or subcellular compartments and allowing experiments at the single live cell or the whole organism level. The discovery of the entire color palette of GFP-like proteins allowed multicolor experiments using a combination of two or more fluorescent probes with different colors. A live cell is a complex biological system, and its proper functioning is highly dependent on intermolecular communication and the coordinated action of diverse molecular constituents. Hence, the development of synchronized probes that simultaneously report on multiple cellular processes allows the spatiotemporal correlation of different activities at the single cell level. The application of two or more fluorophores with different spectral properties or a combination of various FRET pairs is a prerequisite for these so-called multiparameter experiments [27, 139].

As already stated above, the use of YFPs as pH reporters is hampered by the fact that the fluorescence of the protein is also dependent on the halide concentrations. The dual sensitivity to Cl^- and H^+ complicates interpretation of the experiments where both ion concentrations simultaneously change. To overcome these drawbacks, Arosio et al. [140] developed a non-FRET-based sensor, ClopHensor, which simultaneously reports changes in both intracellular Cl^- and H^+ concentrations. A highly specific anion-binding site was engineered in EGFP by the T203Y substitution (E^2GFP) [141]. Ratiometric ClopHensor was developed by the fusion of

E^2GFP to the pH- and Cl^--insensitive DsRed monomer. ClopHensor operates upon excitation at three wavelengths: a 488-nm pH-dependent E^2GFP signal, a 458-nm pH-independent E^2GFP signal, and a 543-nm Cl^-- and pH-independent DsRed signal. Upon Cl^- binding to E^2GFP, a population of nonfluorescent protein is generated with no changes in the ratio between neutral and anionic E^2GFP excitation signals [71]. Therefore, ClopHensor allows independent ratiometric measurements of pH using the green-to-cyan ratio, which is not affected by Cl^- concentrations. At the same time, ratiometric measurements of Cl^- concentrations require pH-dependent calibration curves and occur via the cyan-to-red ratio [140]. The construct exhibits pKa = 6.8 for H^+ and a Kd in the 40–50 mM range for Cl^- at physiological pH [142]. To target the probe to the intracellular large dense-core vesicles (LDCVs), the dominant secretory organelles in neuroendocrine cells, ClopHensor was fused to the N-terminal signal sequence of neuropeptide Y. ClopHensor allowed measurement of the average LDCV pHi, 5.2 ± 0.4. Simultaneously, a high LDCV chloride concentration that varied in the range of 110 mM (s.d., 48 mM) was detected. This variability was tentatively attributed to dynamic changes in the chloride concentration during the exocytosis process [140].

The expression of ClopHensor in hippocampal pyramidal neurons often resulted in a highly heterogeneous expression pattern, with dense intracellular aggregates. This finding was associated with the DsRed susceptibility to aggregation, particularly within fusion proteins. To resolve this problem, Raimondo et al. [143] constructed a new genetically encoded ratiometric Cl^- and pH sensor, ClopHensorN, which was optimized for the nervous system. The DsRed monomer in the original ClopHensor construct was replaced with either mCherry or tandem dimer tomato (tdTomato). Similar to ClopHensor, the E^2GFP-mCherry fusion showed considerable intracellular aggregation. In contrast, the E^2GFP-tdTomato fusion protein exhibited uniform expression of the sensor. The utility of ClopHensorN was demonstrated by measuring activity-dependent ion dynamics in hippocampal neurons [143].

A disadvantage of this approach is that ClopHensorN is an excitation reporter, which implies measurements of the laser excitation intensity and the corresponding corrections to account for independent fluctuations in the power of confocal laser lines. Moreover, pH affects the affinity of ClopHensorN for chloride anions, implying rather complex procedures to correct the Cl^- ratios for concurrent pH fluctuations. Additionally, the ClopHensor probe requires sequential illumination with three wavelengths, which complicates the experimental setup. To simplify the setup requirements, Paredes et al. [144] designed LSSmClopHensor, an optimized version of the ClopHensor sensor. In the LSSmClopHensor construct, the DsRed monomer was substituted for LSSmKate2, a protein with a longer Stokes shift, which allows the use of two excitation wavelengths (458 and 488 nm) instead of three for the whole setup. Later, Sato et al.

[145] used LSSmClopHensor to develop a method for simultaneous two-photon *in vivo* imaging of [Cl⁻]i and pHi in individual cortical pyramidal neurons. Simultaneous measurements of [Cl⁻]i and pHi at the single cell level in the mouse cortex provided direct experimental evidence for the postnatal developmental decrease in intraneuronal Cl^- concentrations and the role of the K^+-Cl^- cotransporter KCC2 in this process. A dynamic two-photon excitation protocol for simultaneous determination of pHi and [Cl⁻]i changes *in vivo* has been provided [145].

The fluorescence of some of GFP-like proteins can be controlled by light of a specific wavelength. This property enables labeling of individual cells, organelles, or proteins and, once the label is activated by light, imaging the movements of the labeled objects is attainable with high spatiotemporal resolution. A highly promising application of these photocontrollable proteins is super-resolution fluorescence microscopy [130]. A photoconvertible FP from *Dendronephthya* sp. (Dend FP) [146] irreversibly changes its emission color from green (506 nm) to red (578 nm) upon illumination with UV or blue light [44]. It was shown that Dend FP manifests a pronounced pH sensitivity and that upon acidification, the photoconverted red form of Dend FP changes its emission color back to green (pKa = 6.24 ± 0.03) [147]. This change in turn provides another opportunity for using Dend FP as a tracking dye and a pH sensor simultaneously. This dual-purpose probe would be very promising for tracking the movements and pH of individual vesicles during endocytosis, cargo sorting and degradation. However, protein oligomerization is a feature that imposes limitations on the use of Dend FP in live cell experiments. Pakhomov et al. [148] used Dendra2, a monomeric version of Dend FP, as a ratiometric genetically encoded pH sensor. Due to protonation of the phenolic group, the red photoconverted form of Dendra2 reversibly turned green upon acidification with a pKa of approximately 7.5. A significant drawback of Dendra2 is the incomplete photoconversion of the protein, resulting in residual green fluorescence that interferes with the green signal of the photoconverted form. To overcome this deficiency, pH imaging was carried out with 360 nm excitation light, as at this wavelength, the unconverted form is nonfluorescent. For live cell studies, two constructs were developed; the first encoded the cytoplasmically localized Dendra2 (cytoDenra2) and the second encoding mitochondria-targeted Dendra2 (mitoDendra2). The cytoplasmic pH in HEK 293 and CHO cells was measured to be 7.40 ± 0.05 for both cell lines, whereas the mitochondrial pH was 8.00 ± 0.07 in HEK 293 cells and 8.15 ± 0.05 in CHO cells.

6. Conclusions and outlook

With the advent of genetically encoded fluorescent probes, we are used to looking at biochemical processes at the single cell level, without any noticeable interference of the regular activities of the live cell. Genetically encoded pH sensors have proven to be indispensable for selective targeting to certain cell types, specific intra/extracellular locations, or a particular subcellular compartment. Although a variety of genetically encoded pH sensors have been designed and applied at the single cell level, there is still much room for improvements in existing pH sensors and future developments of novel and powerful tools for pH imaging. Among the most pressing challenges in this area is the design and application of sensors for tissue or whole-animal experiments. When used in tissues or transgenic animals, the presently available pH sensors suffer from a low signal-to-noise ratio due to their low brightness. Most likely, future engineering of far-red/near-infrared genetically encoded pH sensors with high brightness will solve the problem. In this regard, applications of enzymatic self-labeling SNAP-tag, CLIP-tag, or HALO-tag technologies will potentially allow the use of bright redshifted semisynthetic pH sensors for deep-tissue imaging or whole-body experiments. Effective BRET-based pH sensors also hold great promise, since there is no need for the penetration of excitation light into deep tissues. Although several far-red/near-infrared FPs have become available in the past years, the cyan/yellow FP FRET pair is still the most frequently used sensor for pH imaging in live cells. The development of longer-wavelength FRET-based pH sensors will potentially allow their application in tissues or even in animals as efficiently as in cells.

Another important challenge is the spatiotemporal correlation of pH changes with other cellular events by means of multiparameter imaging. To meet this goal, simultaneous visualization of different cellular activities should be realized by means of a wide range of spectrally distinct single fluorophores or multiple FRET pairs [149]. However, due to the considerable size of most genetically encoded fluorescent sensors, there is a possibility that fusion proteins would not function exactly like their native precursors. For addressing this issue, the development of small peptide tags, such as the tetracysteine tag [150], that specifically bind small-molecule synthetic fluorophores or the use of noncanonical fluorescent amino acids (ncAAs) [151, 152] modified with pH-sensitive fluorophores appears increasingly promising.

Acknowledgements

This work was financially supported by the Russian Science Foundation (grant № 14-50-00131)

References

[1] R. Orij, S. Brul, G.J. Smits, Intracellular pH is a tightly controlled signal in yeast, Bba-Gen Subjects, 1810 (2011) 933-944.
[2] B.A. Webb, M. Chimenti, M.P. Jacobson, D.L. Barber, Dysregulated pH: a perfect storm for cancer progression, Nature reviews. Cancer, 11 (2011) 671-677.
[3] M. Damaghi, J.W. Wojtkowiak, R.J. Gillies, pH sensing and regulation in cancer, Frontiers in physiology, 4 (2013) 370.
[4] P. Swietach, R.D. Vaughan-Jones, A.L. Harris, A. Hulikova, The chemistry, physiology and pathology of pH in cancer, Philos T R Soc B, 369 (2014).
[5] S. Kobayashi, Y. Tanaka, M. Kiyono, M. Chino, T. Chikuma, K. Hoshi, H. Ikeshima, Dependence pH and proposed mechanism for aggregation of Alzheimer's disease-related amyloid-beta(1-42) protein, J Mol Struct, 1094 (2015) 109-117.
[6] C. Stock, A. Schwab, Protons make tumor cells move like clockwork, Pflug Arch Eur J Phy, 458 (2009) 981-992.
[7] W.K. Schmidt, H.P. Moore, Ionic milieu controls the compartment-specific activation of pro-opiomelanocortin processing in AtT-20 cells, Molecular biology of the cell, 6 (1995) 1271-1285.
[8] M.A. Rahman, P. Kumar, D.S. Park, Y.B. Shim, Electrochemical Sensors Based on Organic Conjugated Polymers, Sensors, 8 (2008) 118-141.
[9] X.M. Shi, L.P. Mei, N. Zhang, W.W. Zhao, J.J. Xu, H.Y. Chen, A Polymer Dots-Based Photoelectrochemical pH Sensor: Simplicity, High Sensitivity, and Broad-Range pH Measurement, Anal Chem, 90 (2018) 8300-8303.
[10] S.W. Bishnoi, C.J. Rozell, C.S. Levin, M.K. Gheith, B.R. Johnson, D.H. Johnson, N.J. Halas, All-optical nanoscale pH meter, Nano letters, 6 (2006) 1687-1692.
[11] F. Sun, P. Zhang, T. Bai, D. David Galvan, H.C. Hung, N. Zhou, S. Jiang, Q. Yu, Functionalized plasmonic nanostructure arrays for direct and accurate mapping extracellular pH of living cells in complex media using SERS, Biosens Bioelectron, 73 (2015) 202-207.
[12] D. Wencel, T. Abel, C. McDonagh, Optical chemical pH sensors, Anal Chem, 86 (2014) 15-29.
[13] H. Xu, D. Li, Y. Zhao, X. Wang, D. Li, Y. Wang, Sodium 4-mercaptophenolate capped CdSe/ZnS quantum dots as a fluorescent probe for pH detection in acidic aqueous media, Luminescence, 33 (2018) 410-416.
[14] H. Shen, J. Liu, J. Lei, H. Ju, A core-shell nanoparticle-peptide@metal-organic framework as pH and enzyme dual-recognition switch for stepwise-responsive imaging in living cells, Chem Commun (Camb), 54 (2018) 9155-9158.
[15] A.Q. Zheng, N. Wang, M.L. Chen, Y. Shu, J.H. Wang, Probing pH variation in living cells and assaying hemoglobin in blood with nitrogen enriched carbon dots, Talanta, 188 (2018) 788-794.
[16] J.F. Shangguan, D.G. He, X.X. He, K.M. Wang, F.Z. Xu, J.Q. Liu, J.L. Tang, X. Yang, J. Huang, Label-Free Carbon-Dots-Based Ratiometric Fluorescence pH Nanoprobes for Intracellular pH Sensing, Analytical Chemistry, 88 (2016) 7837-7843.
[17] B. Korzeniowska, R. Woolley, J. DeCourcey, D. Wencel, C.E. Loscher, C. McDonagh, Intracellular pH-Sensing Using Core/Shell Silica Nanoparticles, J Biomed Nanotechnol, 10 (2014) 1336-1345.
[18] W.D. H. Song, C. Liu, Z. Li, H. Zhang, L., M.Y. Wei, Self-Assembled Micellar Nanosensor toward pH with high photo-stability and its application in living cells, Sensors and Actuators: B. Chemical, 273 (2018) 927-934
[19] R. Pal, D. Parker, A ratiometric optical imaging probe for intracellular pH based on modulation of europium emission, Org Biomol Chem, 6 (2008) 1020-1033.
[20] Q. Zhang, M. Zhou, A profluorescent ratiometric probe for intracellular pH imaging, Talanta, 131 (2015) 666-671.

[21] J.Y. Han, K. Burgess, Fluorescent Indicators for Intracellular pH, Chemical reviews, 110 (2010) 2709-2728.
[22] J. Yin, Y. Hu, J. Yoon, Fluorescent probes and bioimaging: alkali metals, alkaline earth metals and pH, Chem Soc Rev, 44 (2015) 4619-4644.
[23] J.T. Hou, W.X. Ren, K. Li, J. Seo, A. Sharma, X.Q. Yu, J.S. Kim, Fluorescent bioimaging of pH: from design to applications, Chem Soc Rev, 46 (2017) 2076-2090.
[24] J. Karagiannis, P.G. Young, Intracellular pH homeostasis during cell-cycle progression and growth state transition in Schizosaccharomyces pombe, J Cell Sci, 114 (2001) 2929-2941.
[25] J.R. Enterina, L. Wu, R.E. Campbell, Emerging fluorescent protein technologies, Current opinion in chemical biology, 27 (2015) 10-17.
[26] D.M. Chudakov, M.V. Matz, S. Lukyanov, K.A. Lukyanov, Fluorescent proteins and their applications in imaging living cells and tissues, Physiol Rev, 90 (2010) 1103-1163.
[27] H.J. Carlson, R.E. Campbell, Genetically encoded FRET-based biosensors for multiparameter fluorescence imaging, Current opinion in biotechnology, 20 (2009) 19-27.
[28] A.A. Pakhomov, V.I. Martynov, GFP family: structural insights into spectral tuning, Chem Biol, 15 (2008) 755-764.
[29] G.S. Baird, D.A. Zacharias, R.Y. Tsien, Biochemistry, mutagenesis, and oligomerization of DsRed, a red fluorescent protein from coral, Proc Natl Acad Sci U S A, 97 (2000) 11984-11989.
[30] R. Bizzarri, M. Serresi, S. Luin, F. Beltram, Green fluorescent protein based pH indicators for in vivo use: a review, Analytical and bioanalytical chemistry, 393 (2009) 1107-1122.
[31] M. Bencina, Illumination of the spatial order of intracellular pH by genetically encoded pH-sensitive sensors, Sensors, 13 (2013) 16736-16758.
[32] A. Martiniere, G. Desbrosses, H. Sentenac, N. Paris, Development and properties of genetically encoded pH sensors in plants, Frontiers in plant science, 4 (2013) 523.
[33] D.P. Barondeau, C.D. Putnam, C.J. Kassmann, J.A. Tainer, E.D. Getzoff, Mechanism and energetics of green fluorescent protein chromophore synthesis revealed by trapped intermediate structures, Proc Natl Acad Sci U S A, 100 (2003) 12111-12116.
[34] L. Zhang, H.N. Patel, J.W. Lappe, R.M. Wachter, Reaction progress of chromophore biogenesis in green fluorescent protein, Journal of the American Chemical Society, 128 (2006) 4766-4772.
[35] N.V. Pletneva, V.Z. Pletnev, K.A. Lukyanov, N.G. Gurskaya, E.A. Goryacheva, V.I. Martynov, A. Wlodawer, Z. Dauter, S. Pletnev, Structural evidence for a dehydrated intermediate in green fluorescent protein chromophore biosynthesis, The Journal of biological chemistry, 285 (2010) 15978-15984.
[36] V. Sample, R.H. Newman, J. Zhang, The structure and function of fluorescent proteins, Chem Soc Rev, 38 (2009) 2852-2864.
[37] A.A. Pakhomov, V.I. Martynov, Posttranslational chemistry of proteins of the GFP family, Biochemistry (Mosc), 74 (2009) 250-259.
[38] L.A. Gross, G.S. Baird, R.C. Hoffman, K.K. Baldridge, R.Y. Tsien, The structure of the chromophore within DsRed, a red fluorescent protein from coral, Proc Natl Acad Sci U S A, 97 (2000) 11990-11995.
[39] A.A. Pakhomov, V.I. Martynov, Chromophore aspartate oxidation-decarboxylation in the green-to-red conversion of a fluorescent protein from Zoanthus sp. 2, Biochemistry, 46 (2007) 11528-11535.
[40] S.J. Remington, R.M. Wachter, D.K. Yarbrough, B. Branchaud, D.C. Anderson, K. Kallio, K.A. Lukyanov, zFP538, a yellow-fluorescent protein from Zoanthus, contains a novel three-ring chromophore, Biochemistry, 44 (2005) 202-212.
[41] N.V. Pletneva, S.V. Pletnev, D.M. Chudakov, T.V. Tikhonova, V.O. Popov, V.I. Martynov, A. Wlodawer, Z. Dauter, V.Z. Pletnev, Three-dimensional structure of yellow fluorescent protein zYFP538 from Zoanthus sp. at the resolution 1.8 Å, Russ J Bioorg Chem, 33 (2007) 390-398.

[42] N. Pletneva, S. Pletnev, T. Tikhonova, V. Popov, V. Martynov, V. Pletnev, Structure of a red fluorescent protein from Zoanthus, zRFP574, reveals a novel chromophore, Acta Crystallogr D Biol Crystallogr, 62 (2006) 527-532.
[43] H. Mizuno, T.K. Mal, K.I. Tong, R. Ando, T. Furuta, M. Ikura, A. Miyawaki, Photo-induced peptide cleavage in the green-to-red conversion of a fluorescent protein, Mol Cell, 12 (2003) 1051-1058.
[44] A.A. Pakhomov, N.Y. Martynova, N.G. Gurskaya, T.A. Balashova, V.I. Martynov, Photoconversion of the chromophore of a fluorescent protein from Dendronephthya sp, Biochemistry (Mosc), 69 (2004) 901-908.
[45] Y.A. Tretyakova, A.A. Pakhomov, V.I. Martynov, Chromophore structure of the kindling fluorescent protein asFP595 from Anemonia sulcata, Journal of the American Chemical Society, 129 (2007) 7748-7749.
[46] P.G. Wilmann, J. Petersen, R.J. Devenish, M. Prescott, J. Rossjohn, Variations on the GFP chromophore: A polypeptide fragmentation within the chromophore revealed in the 2.1-A crystal structure of a nonfluorescent chromoprotein from Anemonia sulcata, The Journal of biological chemistry, 280 (2005) 2401-2404.
[47] M.A. Elsliger, R.M. Wachter, G.T. Hanson, K. Kallio, S.J. Remington, Structural and spectral response of green fluorescent protein variants to changes in pH, Biochemistry, 38 (1999) 5296-5301.
[48] W.W. Ward, H.J. Prentice, A.F. Roth, C.W. Cody, S.C. Reeves, Spectral perturbations of the Aequorea green-fluorescent protein, Photochem Photobiol, 35 (1982) 803-808.
[49] H. Niwa, S. Inouye, T. Hirano, T. Matsuno, S. Kojima, M. Kubota, M. Ohashi, F.I. Tsuji, Chemical nature of the light emitter of the Aequorea green fluorescent protein, Proc Natl Acad Sci U S A, 93 (1996) 13617-13622.
[50] K. Brejc, T.K. Sixma, P.A. Kitts, S.R. Kain, R.Y. Tsien, M. Ormo, S.J. Remington, Structural basis for dual excitation and photoisomerization of the Aequorea victoria green fluorescent protein, Proc Natl Acad Sci U S A, 94 (1997) 2306-2311.
[51] G.J. Palm, A. Zdanov, G.A. Gaitanaris, R. Stauber, G.N. Pavlakis, A. Wlodawer, The structural basis for spectral variations in green fluorescent protein, Nat Struct Biol, 4 (1997) 361-365.
[52] R. Heim, A.B. Cubitt, R.Y. Tsien, Improved green fluorescence, Nature, 373 (1995) 663-664.
[53] H.W. Ai, N.C. Shaner, Z. Cheng, R.Y. Tsien, R.E. Campbell, Exploration of new chromophore structures leads to the identification of improved blue fluorescent proteins, Biochemistry, 46 (2007) 5904-5910.
[54] B.N. Giepmans, S.R. Adams, M.H. Ellisman, R.Y. Tsien, The fluorescent toolbox for assessing protein location and function, Science, 312 (2006) 217-224.
[55] M. Kneen, J. Farinas, Y. Li, A.S. Verkman, Green fluorescent protein as a noninvasive intracellular pH indicator, Biophys J, 74 (1998) 1591-1599.
[56] J. Llopis, J.M. McCaffery, A. Miyawaki, M.G. Farquhar, R.Y. Tsien, Measurement of cytosolic, mitochondrial, and Golgi pH in single living cells with green fluorescent proteins, Proc Natl Acad Sci U S A, 95 (1998) 6803-6808.
[57] G. Miesenbock, D.A. De Angelis, J.E. Rothman, Visualizing secretion and synaptic transmission with pH-sensitive green fluorescent proteins, Nature, 394 (1998) 192-195.
[58] S. Sankaranarayanan, D. De Angelis, J.E. Rothman, T.A. Ryan, The use of pHluorins for optical measurements of presynaptic activity, Biophysical Journal, 79 (2000) 2199-2208.
[59] T. Tsuboi, G.A. Rutter, Multiple forms of "kiss-and-run" exocytosis revealed by evanescent wave microscopy, Curr Biol, 13 (2003) 563-567.
[60] S.P. Gandhi, C.F. Stevens, Three modes of synaptic vesicular recycling revealed by single-vesicle imaging, Nature, 423 (2003) 607-613.

[61] G.A. Yudowski, M.A. Puthenveedu, M. von Zastrow, Distinct modes of regulated receptor insertion to the somatodendritic plasma membrane, Nature neuroscience, 9 (2006) 622-627.
[62] Y. Li, B.D. Roy, W. Wang, L. Zhang, L. Zhang, S.B. Sampson, Y. Yang, D.T. Lin, Identification of two functionally distinct endosomal recycling pathways for dopamine D(2) receptor, The Journal of neuroscience : the official journal of the Society for Neuroscience, 32 (2012) 7178-7190.
[63] D. Jullie, D. Choquet, D. Perrais, Recycling Endosomes Undergo Rapid Closure of a Fusion Pore on Exocytosis in Neuronal Dendrites, Journal of Neuroscience, 34 (2014) 11106-11118.
[64] R.M. Wachter, M.A. Elsliger, K. Kallio, G.T. Hanson, S.J. Remington, Structural basis of spectral shifts in the yellow-emission variants of green fluorescent protein, Structure, 6 (1998) 1267-1277.
[65] M.F. Abad, G. Di Benedetto, P.J. Magalhaes, L. Filippin, T. Pozzan, Mitochondrial pH monitored by a new engineered green fluorescent protein mutant, The Journal of biological chemistry, 279 (2004) 11521-11529.
[66] O. Griesbeck, G.S. Baird, R.E. Campbell, D.A. Zacharias, R.Y. Tsien, Reducing the environmental sensitivity of yellow fluorescent protein. Mechanism and applications, The Journal of biological chemistry, 276 (2001) 29188-29194.
[67] R.M. Wachter, S.J. Remington, Sensitivity of the yellow variant of green fluorescent protein to halides and nitrate, Curr Biol, 9 (1999) R628-629.
[68] M.J. Mahon, pHluorin2: an enhanced, ratiometric, pH-sensitive green florescent protein, Advances in bioscience and biotechnology, 2 (2011) 132-137.
[69] J. Plasek, A. Melcrova, D. Gaskova, Enhanced sensitivity of pHluorin-based monitoring of intracellular pH changes achieved through synchronously scanned fluorescence spectra, Anal Chem, 87 (2015) 9600-9604.
[70] M. Serresi, R. Bizzarri, F. Cardarelli, F. Beltram, Real-time measurement of endosomal acidification by a novel genetically encoded biosensor, Analytical and bioanalytical chemistry, 393 (2009) 1123-1133.
[71] R. Bizzarri, C. Arcangeli, D. Arosio, F. Ricci, P. Faraci, F. Cardarelli, F. Beltram, Development of a novel GFP-based ratiometric excitation and emission pH indicator for intracellular studies, Biophys J, 90 (2006) 3300-3314.
[72] G.T. Hanson, T.B. McAnaney, E.S. Park, M.E. Rendell, D.K. Yarbrough, S. Chu, L. Xi, S.G. Boxer, M.H. Montrose, S.J. Remington, Green fluorescent protein variants as ratiometric dual emission pH sensors. 1. Structural characterization and preliminary application, Biochemistry, 41 (2002) 15477-15488.
[73] F.J. Schmitt, B. Thaa, C. Junghans, M. Vitali, M. Veit, T. Friedrich, eGFP-pHsens as a highly sensitive fluorophore for cellular pH determination by fluorescence lifetime imaging microscopy (FLIM), Biochim Biophys Acta, 1837 (2014) 1581-1593.
[74] A. Battisti, M.A. Digman, E. Gratton, B. Storti, F. Beltram, R. Bizzarri, Intracellular pH measurements made simple by fluorescent protein probes and the phasor approach to fluorescence lifetime imaging, Chem Commun (Camb), 48 (2012) 5127-5129.
[75] M. Chesler, Regulation and modulation of pH in the brain, Physiol Rev, 83 (2003) 1183-1221.
[76] J.A. Wemmie, R.J. Taugher, C.J. Kreple, Acid-sensing ion channels in pain and disease, Nat Rev Neurosci, 14 (2013) 461-471.
[77] M. Chiacchiaretta, S. Latifi, M. Bramini, M. Fadda, A. Fassio, F. Benfenati, F. Cesca, Neuronal hyperactivity causes Na+/H+ exchanger-induced extracellular acidification at active synapses, J Cell Sci, 130 (2017) 1435-1449.
[78] V.V. Belousov, A.F. Fradkov, K.A. Lukyanov, D.B. Staroverov, K.S. Shakhbazov, A.V. Terskikh, S. Lukyanov, Genetically encoded fluorescent indicator for intracellular hydrogen peroxide, Nat Methods, 3 (2006) 281-286.

[79] D. Poburko, J. Santo-Domingo, N. Demaurex, Dynamic regulation of the mitochondrial proton gradient during cytosolic calcium elevations, The Journal of biological chemistry, 286 (2011) 11672-11684.
[80] M.E. Matlashov, Y.A. Bogdanova, G.V. Ermakova, N.M. Mishina, Y.G. Ermakova, E.S. Nikitin, P.M. Balaban, S. Okabe, S. Lukyanov, G. Enikolopov, A.G. Zaraisky, V.V. Belousov, Fluorescent ratiometric pH indicator SypHer2: Applications in neuroscience and regenerative biology, Biochim Biophys Acta, 1850 (2015) 2318-2328.
[81] M.V. Shirmanova, I.N. Druzhkova, M.M. Lukina, M.E. Matlashov, V.V. Belousov, L.B. Snopova, N.N. Prodanetz, V.V. Dudenkova, S.A. Lukyanov, E.V. Zagaynova, Intracellular pH imaging in cancer cells in vitro and tumors in vivo using the new genetically encoded sensor SypHer2, Biochim Biophys Acta, 1850 (2015) 1905-1911.
[82] Y.G. Ermakova, V.V. Pak, Y.A. Bogdanova, A.A. Kotlobay, I.V. Yampolsky, A.G. Shokhina, A.S. Panova, R.A. Marygin, D.B. Staroverov, D.S. Bilan, H. Sies, V.V. Belousov, SypHer3s: a genetically encoded fluorescent ratiometric probe with enhanced brightness and an improved dynamic range, Chem Commun (Camb), 54 (2018) 2898-2901.
[83] R. Heim, R.Y. Tsien, Engineering green fluorescent protein for improved brightness, longer wavelengths and fluorescence resonance energy transfer, Curr Biol, 6 (1996) 178-182.
[84] M.V. Matz, A.F. Fradkov, Y.A. Labas, A.P. Savitsky, A.G. Zaraisky, M.L. Markelov, S.A. Lukyanov, Fluorescent proteins from nonbioluminescent Anthozoa species, Nat Biotechnol, 17 (1999) 969-973.
[85] M. Rajendran, B. Claywell, E.P. Haynes, U. Scales, C.K. Henning, M. Tantama, Imaging pH Dynamics Simultaneously in Two Cellular Compartments Using a Ratiometric pH-Sensitive Mutant of mCherry, ACS omega, 3 (2018) 9476-9486.
[86] R.E. Campbell, O. Tour, A.E. Palmer, P.A. Steinbach, G.S. Baird, D.A. Zacharias, R.Y. Tsien, A monomeric red fluorescent protein, Proc Natl Acad Sci U S A, 99 (2002) 7877-7882.
[87] N.C. Shaner, R.E. Campbell, P.A. Steinbach, B.N. Giepmans, A.E. Palmer, R.Y. Tsien, Improved monomeric red, orange and yellow fluorescent proteins derived from Discosoma sp. red fluorescent protein, Nat Biotechnol, 22 (2004) 1567-1572.
[88] L. Wang, W.C. Jackson, P.A. Steinbach, R.Y. Tsien, Evolution of new nonantibody proteins via iterative somatic hypermutation, Proc Natl Acad Sci U S A, 101 (2004) 16745-16749.
[89] X. Shu, N.C. Shaner, C.A. Yarbrough, R.Y. Tsien, S.J. Remington, Novel chromophores and buried charges control color in mFruits, Biochemistry, 45 (2006) 9639-9647.
[90] D.E. Johnson, H.W. Ai, P. Wong, J.D. Young, R.E. Campbell, J.R. Casey, Red fluorescent protein pH biosensor to detect concentrative nucleoside transport, The Journal of biological chemistry, 284 (2009) 20499-20511.
[91] Y. Li, R.W. Tsien, pHTomato, a red, genetically encoded indicator that enables multiplex interrogation of synaptic activity, Nature neuroscience, 15 (2012) 1047-1053.
[92] N.C. Shaner, M.Z. Lin, M.R. McKeown, P.A. Steinbach, K.L. Hazelwood, M.W. Davidson, R.Y. Tsien, Improving the photostability of bright monomeric orange and red fluorescent proteins, Nat Methods, 5 (2008) 545-551.
[93] H. Li, S.M. Foss, Y.L. Dobryy, C.K. Park, S.A. Hires, N.C. Shaner, R.Y. Tsien, L.C. Osborne, S.M. Voglmaier, Concurrent imaging of synaptic vesicle recycling and calcium dynamics, Frontiers in molecular neuroscience, 4 (2011) 34.
[94] G.J. Kremers, K.L. Hazelwood, C.S. Murphy, M.W. Davidson, D.W. Piston, Photoconversion in orange and red fluorescent proteins, Nat Methods, 6 (2009) 355-358.
[95] Y. Shen, M. Rosendale, R.E. Campbell, D. Perrais, pHuji, a pH-sensitive red fluorescent protein for imaging of exo- and endocytosis, The Journal of cell biology, 207 (2014) 419-432.
[96] M. Tantama, Y.P. Hung, G. Yellen, Imaging intracellular pH in live cells with a genetically encoded red fluorescent protein sensor, Journal of the American Chemical Society, 133 (2011) 10034-10037.

[97] J. Berg, Y.P. Hung, G. Yellen, A genetically encoded fluorescent reporter of ATP:ADP ratio, Nat Methods, 6 (2009) 161-166.
[98] T. Awaji, A. Hirasawa, H. Shirakawa, G. Tsujimoto, S. Miyazaki, Novel green fluorescent protein-based ratiometric indicators for monitoring pH in defined intracellular microdomains, Biochem Biophys Res Commun, 289 (2001) 457-462.
[99] C.J. Rosado, D. Mijaljica, I. Hatzinisiriou, M. Prescott, R.J. Devenish, Rosella: a fluorescent pH-biosensor for reporting vacuolar turnover of cytosol and organelles in yeast, Autophagy, 4 (2008) 205-213.
[100] M. Koivusalo, C. Welch, H. Hayashi, C.C. Scott, M. Kim, T. Alexander, N. Touret, K.M. Hahn, S. Grinstein, Amiloride inhibits macropinocytosis by lowering submembranous pH and preventing Rac1 and Cdc42 signaling, The Journal of cell biology, 188 (2010) 547-563.
[101] E.F. Corbett-Nelson, D. Mason, J.G. Marshall, Y. Collette, S. Grinstein, Signaling-dependent immobilization of acylated proteins in the inner monolayer of the plasma membrane, The Journal of cell biology, 174 (2006) 255-265.
[102] K.S. Gjetting, C.K. Ytting, A. Schulz, A.T. Fuglsang, Live imaging of intra- and extracellular pH in plants using pHusion, a novel genetically encoded biosensor, Journal of experimental botany, 63 (2012) 3207-3218.
[103] D. Gao, M.R. Knight, A.J. Trewavas, B. Sattelmacher, C. Plieth, Self-reporting Arabidopsis expressing pH and [Ca2+] indicators unveil ion dynamics in the cytoplasm and in the apoplast under abiotic stress, Plant physiology, 134 (2004) 898-908.
[104] S. Kimura, T. Noda, T. Yoshimori, Dissection of the autophagosome maturation process by a novel reporter protein, tandem fluorescent-tagged LC3, Autophagy, 3 (2007) 452-460.
[105] E. Tresse, F.A. Salomons, J. Vesa, L.C. Bott, V. Kimonis, T.P. Yao, N.P. Dantuma, J.P. Taylor, VCP/p97 is essential for maturation of ubiquitin-containing autophagosomes and this function is impaired by mutations that cause IBMPFD, Autophagy, 6 (2010) 217-227.
[106] G. Maulucci, M. Chiarpotto, M. Papi, D. Samengo, G. Pani, M. De Spirito, Quantitative analysis of autophagic flux by confocal pH-imaging of autophagic intermediates, Autophagy, 11 (2015) 1905-1916.
[107] C. Zhou, W. Zhong, J. Zhou, F. Sheng, Z. Fang, Y. Wei, Y. Chen, X. Deng, B. Xia, J. Lin, Monitoring autophagic flux by an improved tandem fluorescent-tagged LC3 (mTagRFP-mWasabi-LC3) reveals that high-dose rapamycin impairs autophagic flux in cancer cells, Autophagy, 8 (2012) 1215-1226.
[108] S. Tanaka, H. Harada, M. Hiraoka, A novel method to visually determine the intracellular pH of xenografted tumor in vivo by utilizing fluorescent protein as an indicator, Biochem Biophys Res Commun, 464 (2015) 1151-1156.
[109] T. Nagai, K. Ibata, E.S. Park, M. Kubota, K. Mikoshiba, A. Miyawaki, A variant of yellow fluorescent protein with fast and efficient maturation for cell-biological applications, Nat Biotechnol, 20 (2002) 87-90.
[110] J.R. Casey, S. Grinstein, J. Orlowski, Sensors and regulators of intracellular pH, Nature reviews. Molecular cell biology, 11 (2010) 50-61.
[111] R.N. Day, M.W. Davidson, Fluorescent proteins for FRET microscopy: monitoring protein interactions in living cells, Bioessays, 34 (2012) 341-350.
[112] A. Esposito, M. Gralle, M.A. Dani, D. Lange, F.S. Wouters, pHlameleons: a family of FRET-based protein sensors for quantitative pH imaging, Biochemistry, 47 (2008) 13115-13126.
[113] S. Shimozono, H. Hosoi, H. Mizuno, T. Fukano, T. Tahara, A. Miyawaki, Concatenation of cyan and yellow fluorescent proteins for efficient resonance energy transfer, Biochemistry, 45 (2006) 6267-6271.
[114] M.L. Markwardt, G.J. Kremers, C.A. Kraft, K. Ray, P.J. Cranfill, K.A. Wilson, R.N. Day, R.M. Wachter, M.W. Davidson, M.A. Rizzo, An improved cerulean fluorescent protein with enhanced brightness and reduced reversible photoswitching, PLoS One, 6 (2011) e17896.

[115] J. Goedhart, D. von Stetten, M. Noirclerc-Savoye, M. Lelimousin, L. Joosen, M.A. Hink, L. van Weeren, T.W. Gadella, Jr., A. Royant, Structure-guided evolution of cyan fluorescent proteins towards a quantum yield of 93%, Nature communications, 3 (2012) 751.
[116] M. Erard, A. Fredj, H. Pasquier, D.B. Beltolngar, Y. Bousmah, V. Derrien, P. Vincent, F. Merola, Minimum set of mutations needed to optimize cyan fluorescent proteins for live cell imaging, Molecular bioSystems, 9 (2013) 258-267.
[117] F. Merola, A. Fredj, D.B. Betolngar, C. Ziegler, M. Erard, H. Pasquier, Newly engineered cyan fluorescent proteins with enhanced performances for live cell FRET imaging, Biotechnology journal, 9 (2014) 180-191.
[118] D.B. Betolngar, M. Erard, H. Pasquier, Y. Bousmah, A. Diop-Sy, E. Guiot, P. Vincent, F. Merola, pH sensitivity of FRET reporters based on cyan and yellow fluorescent proteins, Analytical and bioanalytical chemistry, 407 (2015) 4183-4193.
[119] B. Liu, S.N. Mavrova, J. van den Berg, S.K. Kristensen, L. Mantovanelli, L.M. Veenhoff, B. Poolman, A.J. Boersma, The influence of fluorescent protein maturation on FRET measurements in living cells, ACS sensors, (2018) doi: 10.1021/acssensors.1028b00473.
[120] A. Wang, J. Feng, Y. Li, P. Zou, Beyond Fluorescent Proteins: Hybrid and Bioluminescent Indicators for Imaging Neural Activities, ACS chemical neuroscience, (2018).
[121] M. Martineau, A. Somasundaram, J.B. Grimm, T.D. Gruber, D. Choquet, J.W. Taraska, L.D. Lavis, D. Perrais, Semisynthetic fluorescent pH sensors for imaging exocytosis and endocytosis, Nature communications, 8 (2017) 1412.
[122] J.B. Grimm, A.J. Sung, W.R. Legant, P. Hulamm, S.M. Matlosz, E. Betzig, L.D. Lavis, Carbofluoresceins and carborhodamines as scaffolds for high-contrast fluorogenic probes, ACS chemical biology, 8 (2013) 1303-1310.
[123] J.B. Grimm, T.D. Gruber, G. Ortiz, T.A. Brown, L.D. Lavis, Virginia Orange: A Versatile, Red-Shifted Fluorescein Scaffold for Single- and Dual-Input Fluorogenic Probes, Bioconjug Chem, 27 (2016) 474-480.
[124] A. Keppler, H. Pick, C. Arrivoli, H. Vogel, K. Johnsson, Labeling of fusion proteins with synthetic fluorophores in live cells, Proc Natl Acad Sci U S A, 101 (2004) 9955-9959.
[125] A.M. Dennis, W.J. Rhee, D. Sotto, S.N. Dublin, G. Bao, Quantum dot-fluorescent protein FRET probes for sensing intracellular pH, ACS nano, 6 (2012) 2917-2924.
[126] I.L. Medintz, H. Mattoussi, Quantum dot-based resonance energy transfer and its growing application in biology, Physical chemistry chemical physics : PCCP, 11 (2009) 17-45.
[127] I.L. Medintz, T. Pons, J.B. Delehanty, K. Susumu, F.M. Brunel, P.E. Dawson, H. Mattoussi, Intracellular delivery of quantum dot-protein cargos mediated by cell penetrating peptides, Bioconjug Chem, 19 (2008) 1785-1795.
[128] T. Drepper, T. Eggert, F. Circolone, A. Heck, U. Krauss, J.K. Guterl, M. Wendorff, A. Losi, W. Gartner, K.E. Jaeger, Reporter proteins for in vivo fluorescence without oxygen, Nat Biotechnol, 25 (2007) 443-445.
[129] C. Rupprecht, M. Wingen, J. Potzkei, T. Gensch, K.E. Jaeger, T. Drepper, A novel FbFP-based biosensor toolbox for sensitive in vivo determination of intracellular pH, Journal of biotechnology, 258 (2017) 25-32.
[130] S.W. Hell, Far-field optical nanoscopy, Science, 316 (2007) 1153-1158.
[131] D.S. Richardson, C. Gregor, F.R. Winter, N.T. Urban, S.J. Sahl, K.I. Willig, S.W. Hell, SRpHi ratiometric pH biosensors for super-resolution microscopy, Nature communications, 8 (2017) 577.
[132] Y. Zhang, Q. Xie, J.B. Robertson, C.H. Johnson, pHlash: a new genetically encoded and ratiometric luminescence sensor of intracellular pH, PLoS One, 7 (2012) e43072.
[133] Y. Zhang, J.B. Robertson, Q. Xie, C.H. Johnson, Monitoring Intracellular pH Change with a Genetically Encoded and Ratiometric Luminescence Sensor in Yeast and Mammalian Cells, Methods Mol Biol, 1461 (2016) 117-130.

[134] A.M. Loening, T.D. Fenn, A.M. Wu, S.S. Gambhir, Consensus guided mutagenesis of Renilla luciferase yields enhanced stability and light output, Protein Eng Des Sel, 19 (2006) 391-400.
[135] T. Nagai, S. Yamada, T. Tominaga, M. Ichikawa, A. Miyawaki, Expanded dynamic range of fluorescent indicators for Ca2+ by circularly permuted yellow fluorescent proteins, P Natl Acad Sci USA, 101 (2004) 10554-10559.
[136] L.A. Perkins, Q. Yan, B.F. Schmidt, D. Kolodieznyi, S. Saurabh, M.B. Larsen, S.C. Watkins, L. Kremer, M.P. Bruchez, Genetically Targeted Ratiometric and Activated pH Indicator Complexes (TRApHIC) for Receptor Trafficking, Biochemistry, 57 (2018) 861-871.
[137] C. Szent-Gyorgyi, B.F. Schmidt, Y. Creeger, G.W. Fisher, K.L. Zakel, S. Adler, J.A. Fitzpatrick, C.A. Woolford, Q. Yan, K.V. Vasilev, P.B. Berget, M.P. Bruchez, J.W. Jarvik, A. Waggoner, Fluorogen-activating single-chain antibodies for imaging cell surface proteins, Nat Biotechnol, 26 (2008) 235-240.
[138] Q. Yan, B.F. Schmidt, L.A. Perkins, M. Naganbabu, S. Saurabh, S.K. Andreko, M.P. Bruchez, Near-instant surface-selective fluorogenic protein quantification using sulfonated triarylmethane dyes and fluorogen activating proteins, Org Biomol Chem, 13 (2015) 2078-2086.
[139] C. Schultz, A. Schleifenbaum, J. Goedhart, T.W. Gadella, Jr., Multiparameter imaging for the analysis of intracellular signaling, Chembiochem, 6 (2005) 1323-1330.
[140] D. Arosio, F. Ricci, L. Marchetti, R. Gualdani, L. Albertazzi, F. Beltram, Simultaneous intracellular chloride and pH measurements using a GFP-based sensor, Nat Methods, 7 (2010) 516-518.
[141] D. Arosio, G. Garau, F. Ricci, L. Marchetti, R. Bizzarri, R. Nifosi, F. Beltram, Spectroscopic and structural study of proton and halide ion cooperative binding to gfp, Biophys J, 93 (2007) 232-244.
[142] M. Mukhtarov, L. Liguori, T. Waseem, F. Rocca, S. Buldakova, D. Arosio, P. Bregestovski, Calibration and functional analysis of three genetically encoded Cl(-)/pH sensors, Frontiers in molecular neuroscience, 6 (2013) 9.
[143] J.V. Raimondo, B. Joyce, L. Kay, T. Schlagheck, S.E. Newey, S. Srinivas, C.J. Akerman, A genetically-encoded chloride and pH sensor for dissociating ion dynamics in the nervous system, Front Cell Neurosci, 7 (2013) 202.
[144] J.M. Paredes, A.I. Idilli, L. Mariotti, G. Losi, L.R. Arslanbaeva, S.S. Sato, P. Artoni, J. Szczurkowska, L. Cancedda, G.M. Ratto, G. Carmignoto, D. Arosio, Synchronous Bioimaging of Intracellular pH and Chloride Based on LSS Fluorescent Protein, ACS chemical biology, 11 (2016) 1652-1660.
[145] S. Sulis Sato, P. Artoni, S. Landi, O. Cozzolino, R. Parra, E. Pracucci, F. Trovato, J. Szczurkowska, S. Luin, D. Arosio, F. Beltram, L. Cancedda, K. Kaila, G.M. Ratto, Simultaneous two-photon imaging of intracellular chloride concentration and pH in mouse pyramidal neurons in vivo, Proc Natl Acad Sci U S A, 114 (2017) E8770-E8779.
[146] Y.A. Labas, N.G. Gurskaya, Y.G. Yanushevich, A.F. Fradkov, K.A. Lukyanov, S.A. Lukyanov, M.V. Matz, Diversity and evolution of the green fluorescent protein family, Proc Natl Acad Sci U S A, 99 (2002) 4256-4261.
[147] A.A. Pakhomov, R.V. Chertkova, V.I. Martynov, pH-sensor properties of a fluorescent protein from Dendronephthya sp., Russ J Bioorg Chem+, 41 (2015) 602-606.
[148] A.A. Pakhomov, V.I. Martynov, A.N. Orsa, A.A. Bondarenko, R.V. Chertkova, K.A. Lukyanov, A.G. Petrenko, I.E. Deyev, Fluorescent protein Dendra2 as a ratiometric genetically encoded pH-sensor, Biochem Biophys Res Commun, 493 (2017) 1518-1521.
[149] A. Piljic, C. Schultz, Simultaneous recording of multiple cellular events by FRET, ACS chemical biology, 3 (2008) 156-160.
[150] S.R. Adams, R.E. Campbell, L.A. Gross, B.R. Martin, G.K. Walkup, Y. Yao, J. Llopis, R.Y. Tsien, New biarsenical ligands and tetracysteine motifs for protein labeling in vitro and in

vivo: synthesis and biological applications, Journal of the American Chemical Society, 124 (2002) 6063-6076.
[151] T.P. Krogager, R.J. Ernst, T.S. Elliott, L. Calo, V. Beranek, E. Ciabatti, M.G. Spillantini, M. Tripodi, M.H. Hastings, J.W. Chin, Labeling and identifying cell-specific proteomes in the mouse brain, Nat Biotechnol, 36 (2018) 156-159.
[152] J. Xie, P.G. Schultz, A chemical toolkit for proteins--an expanded genetic code, Nature reviews. Molecular cell biology, 7 (2006) 775-782.

Table 1. GFP-based single protein nonratiometric pH indicators

Fluorescent protein	Absorbance/Excitation maximum, nm	Emission maximum, nm	Extinction coefficient, M -1 cm -1	Quantum yield	pKa	Refs
EGFP (GFP mutant F64L/S65T)	390,490/490	510	5.5×10^4 (488 nm)	0.6	6.0	[55]
EYFP (S65G/S72A/T203Y/H231L)	390,514/514	527	8.34×10^4 (514 nm)	0.61	7.1	[56]
Ecliptic pHluorin (S147D, N149Q, T161I, S202F, Q204T, A206T)	395,475	508	4.4×10^4 (475 nm)	0.08	7.2	[57]
Superecliptic pHluorin (S147D, N149Q, T161I, S202F, Q204T, A206T, F64L, S65T)	495	512	nd[a]	nd	7.11	[58]

[a] –not determined

Table 2. Ratiometric single protein GFP-based pH indicators

Fluorescent protein	Type	Excitation maximum 1, nm	Excitation maximum 2, nm	Emission maximum 1, nm	Emission maximum 2, nm	pKa	Refs
Ratiometric pHluorin (GFP mutant S202H, E132D, S147E, N149L, N164I, K166Q, I167V, R168H, L220F)	Dual excitation	395	475	508		6.9	[57]
E^2GFP (GFP mutant F64L, S65T, T203Y, L231H)	Dual excitation Dual emission	408	473	508	523	7.0	[71]
deGFP1 (GFP mutant S65T/H148G/T203C)	Dual emission	~400	~508	~460	~515	8.0	[72]
deGFP4 (GFP mutant S65T/C48S/H148C/T203C)	Dual emission	~400	~508	~460	~515	7.3	[72]
SypHer3s (HyPer mutant C199S, Y145F, D129G, Q197L)	Dual excitation	410	495	525	-	7.8	[82]

Table 3. Redshifted single protein pH indicators

Fluorescent protein	Type	Absorbance/Excitation maximum, nm	Emission maximum, nm	Extinction coefficient, M -1 cm -1	Quantum yield	pKa	Refs
mNectarine (mRFP1 mutant Q66C/T147S/Q213L)	Intensiometric	558	578	5.8×10^4 (pH 8.0)	0.45	6.9	[90]
pHTomato (mStrawberry mutant F41T, F83L, S182K, I194K, V195T and G196D)	Intensiometric	550	580	7.05×10^4	0.68	7.8	[91]
mOrange	Intensiometric	548	562	7.1×10^4	0.69	7.5	[92]
mOrange2	Intensiometric	549	565	5.8×10^4	0.60	6.5	[92]
pHuji (mApple mutant K163Y)	Intensiometric	566	598	3.1×10^4	0.22	7.7	[95]
pHRed (mKeima mutant A213S)	Ratiometric, dual excitation	440, 585	610	1.65×10^4 [a]	0.11 [a]	7.8	[96]

[a] – determined at 440 nm, pH 7.0

Table 4. Ratiometric dual protein pH indicators

Name (Fluorophore 1, reference or donor FP)	Fluorophore 2 (pH sensitive or acceptor FP)	Type	Excitation maximum 1, nm	Excitation maximum 2, nm	Emission maximum 1, nm	Emission maximum 2, nm	pKa	Refs
GFpH (GFPuv)	EGFP	Dual excitation	380	480	509	511	6.1	[98]
Rosella (DsRed.T3, reference)	Superecliptic pHluorin	Dual emission		488	587	508	7.11	[99]
mCherry, reference	Superecliptic pHluorin	Dual emission		488	583	508	7.2	[100]
pHusion (mRFP1, reference)	EGFP	Dual emission		488	607	510	5.8	[102]
YFpH, GFPuv (FRET donor)	EYFP (FRET acceptor)	Dual excitation, dual emission FRET-based	380	480	509	527	6.8	[98]
pHlameleon 5, Cy11.5 (ECFP, FRET donor)	YFP Venus (FRET acceptor)	FRET-based	458		474	528	4.8	[112]
pHlameleon 6 (ECFP, FRET donor)	EYFP (FRET acceptor)	FRET-based	458		474	528	6.2	[112]
pHlameleon 7 (ECFP, FRET donor)	YFP H148G (FRET acceptor)	FRET-based	458		474	528	7.1	[112]

Table 5. Hybrid pH sensors

Name Fluorophore 1	Fluorophore 2	Type	Excitation maximum 1, nm	Excitation maximum 2, nm	Emission maximum 1, nm	Emission maximum 2, nm	pKa	Refs
Semisynthetic Carbofluorescein –SNAP-tag conjugate		Intensiometric	544		567		7.5	[121]
Semisynthetic Virginia orange –SNAP-tag conjugate		Intensiometric	555		581		6.7	[121]
Quantum dot-mOrange conjugate (Quantum dot, FRET donor)	mOrange (FRET acceptor)	FRET-based			520	560	6.9	[125]
Quantum dot-mOrange M163K conjugate (Quantum dot, FRET donor)	mOrange M163K (FRET acceptor)	FRET-based	400		520	560	7.9	[125]
FluBpH, FMN-binding protein – EYFP tandems (FMN-binding protein, FRET donor)	EYFP variants (FRET acceptor) Citrine EYFP-L68V EYFP-H148G	FRET-based	380		495	527	5.7 6.1 7.5	[129]
pHlash, Renilla luciferase RLuc8 - circularly permuted Venus FP tandem (RLuc8 BRET donor)	cpVenus FP (BRET acceptor)	BRET-based	-	-	525	475	nd	[132, 133]

Figure legends

Figure 1. Representative chromophore structures of GFP-like proteins. The conjugated π-electron system responsible for the optical properties of the corresponding protein is shaded in color.

Figure 2. Chromophore protonation states and optical properties of GFP-like proteins. A. The protonation equilibrium of the chromophore of wt avGFP. B. The ground state absorption (blue) and emission (green) spectra of wt avGFP. C. Excited state proton transfer (ESPT) in avGFP. The half-round arrow indicates the proton transfer pathway upon absorption of 405 nm light.

Figure 3. Schematic representation of the main types of genetically encoded fluorescent pH indicators. **A.** Nonratiometric FP-based pH indicator. This kind of pH indicators changes intensity at a given excitation or emission wavelength in response to pH variations. **B.** Ratiometric single-protein pH indicator. With ratiometric indicators, the fluorescence intensity ratios (excitation or emission) at two different wavelengths are measured (dual excitation indicator is shown). **C.** Ratiometric dual-FP-based pH indicator. This kind of indicators consists of a fusion of two proteins, one of which is a nonratiometric intensity-based pH-sensitive FP (green) and the other one is a pH-insensitive protein used as a reference (red). **D.** Dual protein FRET-based pH indicator. FRET efficiency between two FPs changes when pH alters.

Figure 4. Dual color imaging of synaptic connection with genetically encoded sensors, pH-sensor sypHTomato (red) and Ca^{2+} sensor GCaMP3 (green). **A.** Image of a pair of connected neurons where pre- and postsynaptic neurons expressed sypHTomato (red) and GCaMP3 (green). Regions 1–6 show putative synapses. Scale bar, 10 μm. **B.** Enlarged views of regions 2, 5 and 6 illustrating morphology and close proximity between presynaptic boutons (red) and postsynaptic spines (green). Intensity distributions along scan lines (dotted) plotted below. Scale bars, 1 μm. Adapted with permission from ref. [90] © (2012) Springer Nature.

Figure 5. Hybrid pH sensors. **A.** Genetically encoded SNAP tag specifically self-labelled with the pH-sensitive benzylguanine derivative of carbofluorescein. **B.** FRET-based pH sensor composed of tandemly fused FMN-binding fluorescent protein and EYFP variants. **C.** BRET-

based pH sensor composed of Renilla luciferase, RLuc8 (BRET donor), and circularly permuted Venus FP (BRET acceptor).

Highlights

- Fluorescent protein (FP)-based pH indicators, advantages and shortcomings
- Redshifted FP-based pH indicators overcome cellular autofluorescence
- FRET-based pH indicators as ratiometric pH-sensing probes
- Hybrid pH sensors combine capabilities of non-GFP fluorophores with advantages of genetically encoded tags

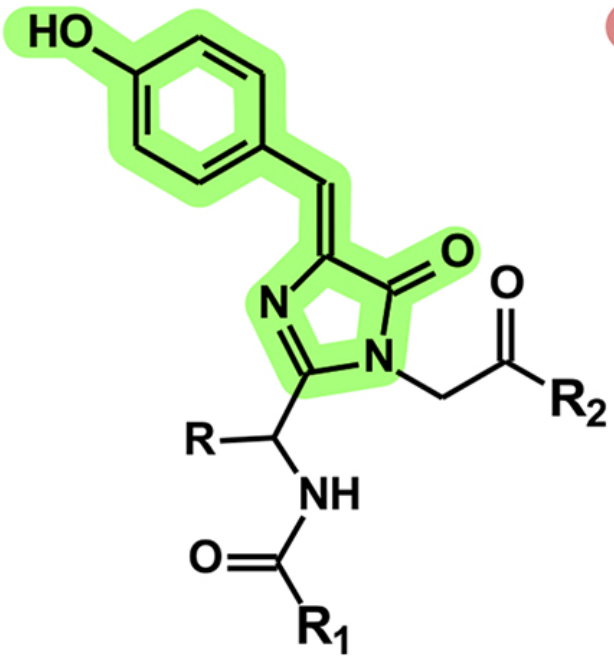

GFP

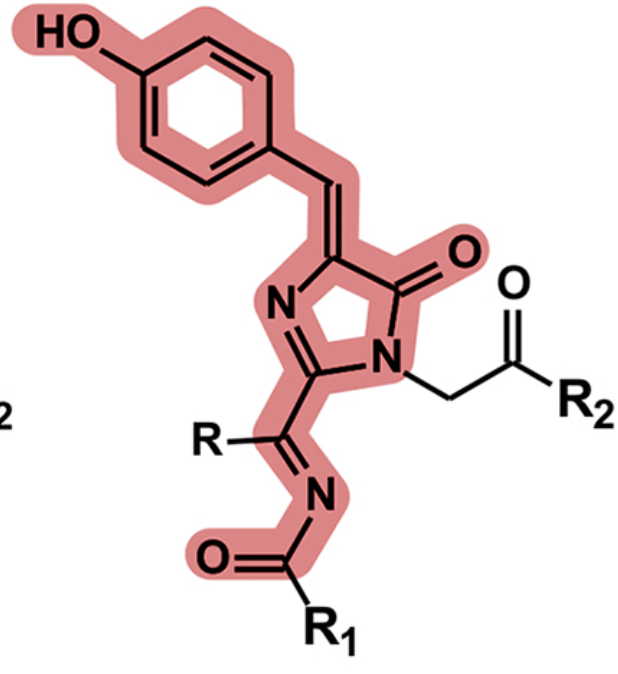

DsRed

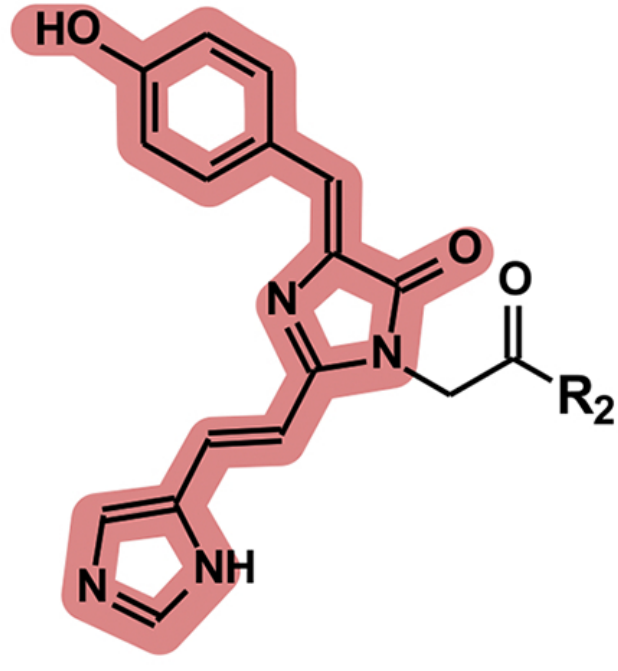

Kaede

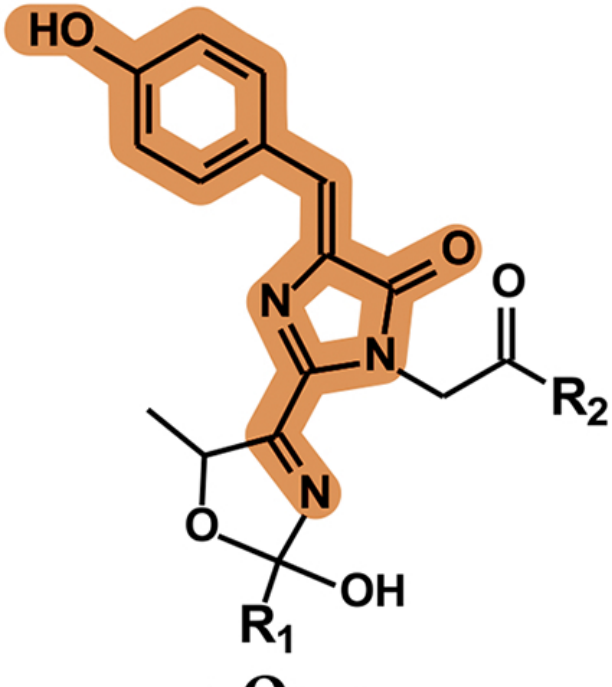

mOrange

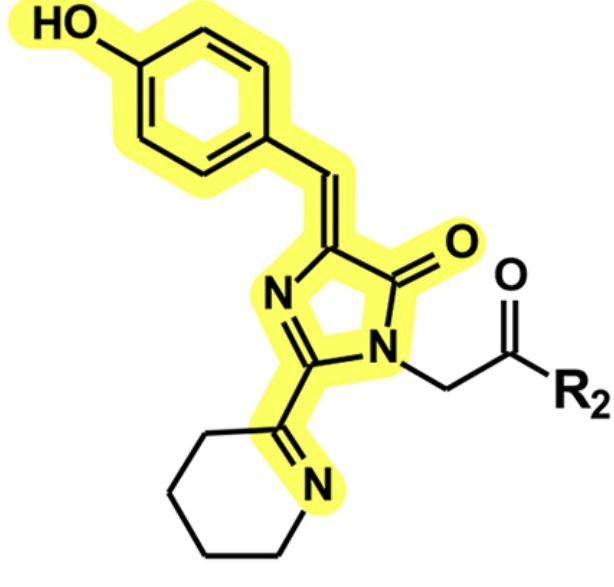

zFP538

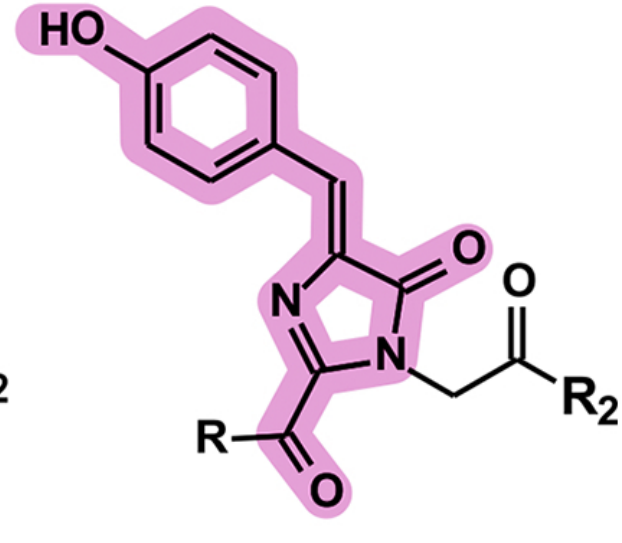

asFP595

Figure 1

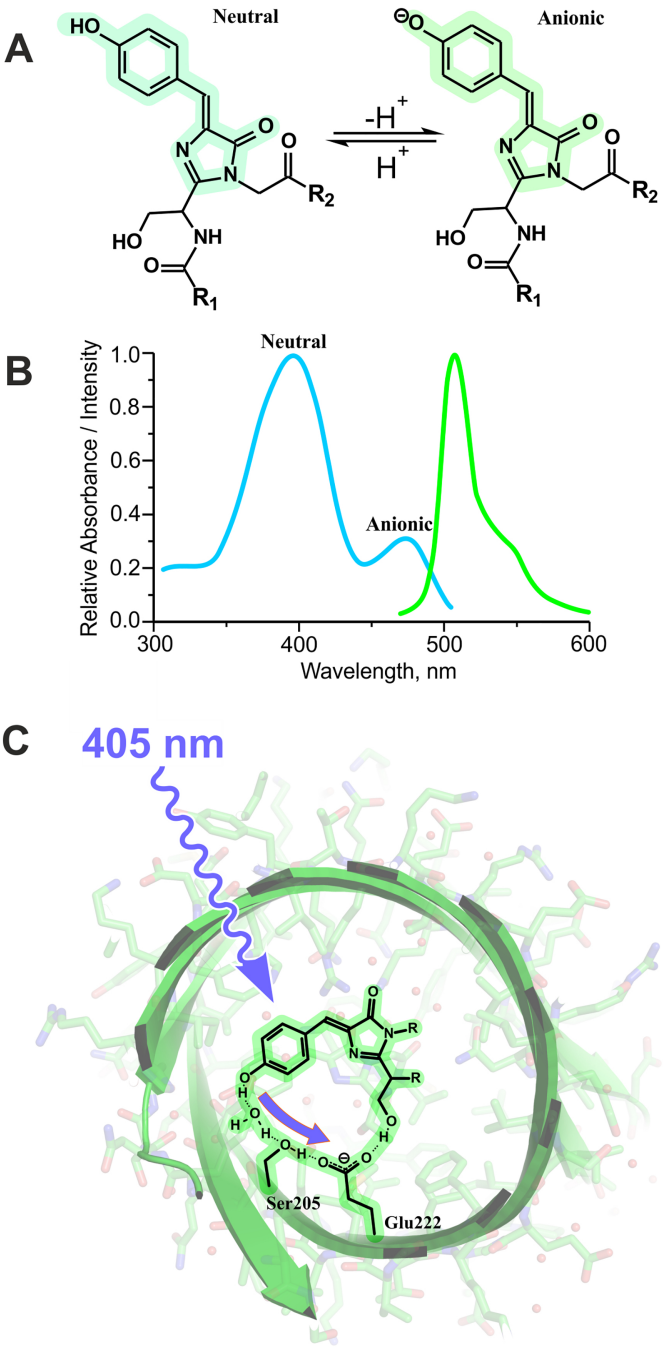
A
Neutral
Anionic
HO
-H+
H+
R2
R1
NH
B
Neutral
Anionic
Relative Absorbance / Intensity
1.0
0.8
0.6
0.4
0.2
0.0
300
400
500
600
Wavelength, nm
C
405 nm
Ser205
Glu222

Figure 2

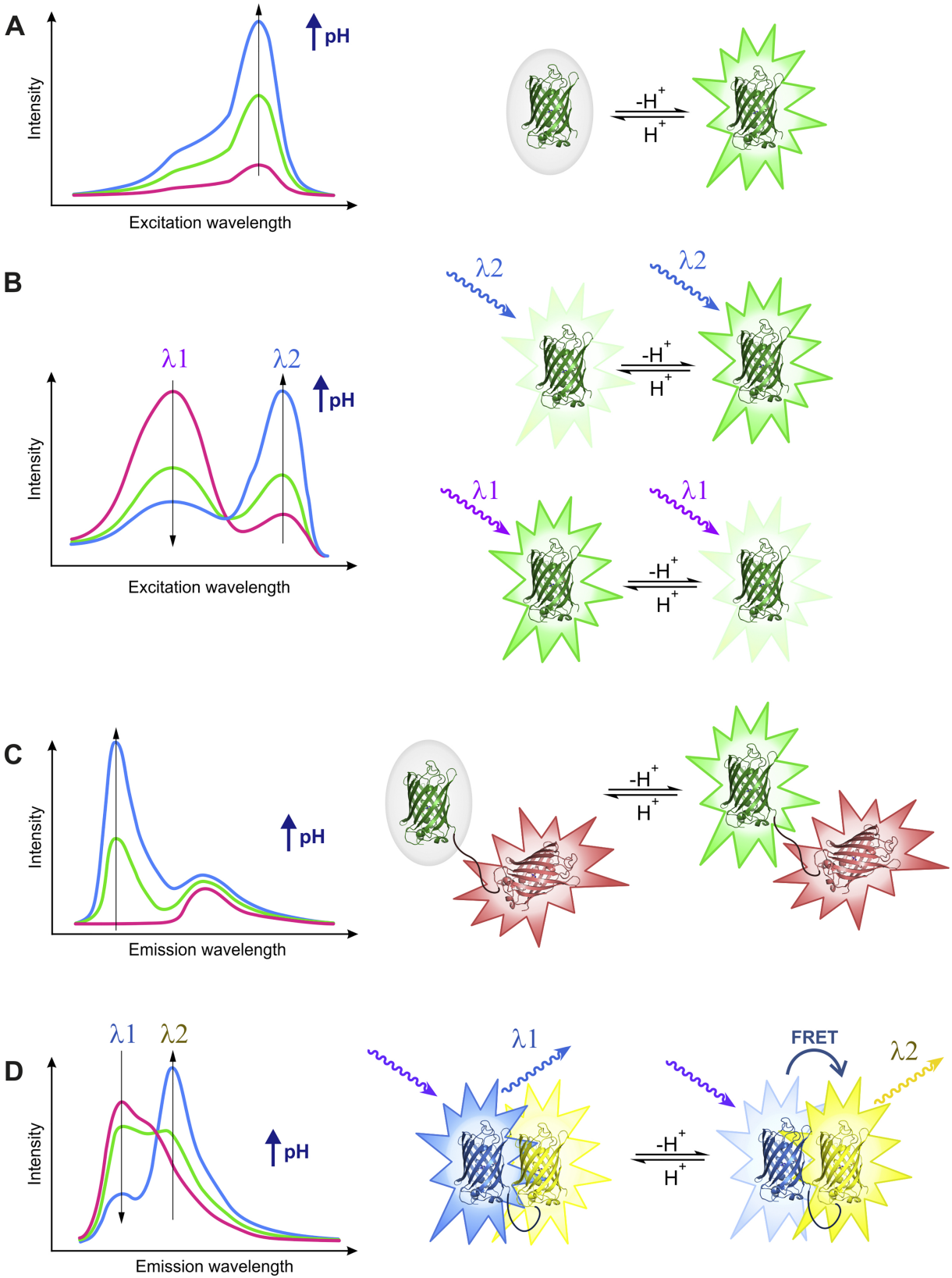
A
Intensity
pH
Excitation wavelength
-H+
H+
B
λ1
λ2
Intensity
pH
Excitation wavelength
λ2
λ2
-H+
H+
λ1
λ1
-H+
H+
C
Intensity
pH
Emission wavelength
-H+
H+
D
λ1
λ2
Intensity
pH
Emission wavelength
λ1
FRET
λ2
-H+
H+

Figure 3

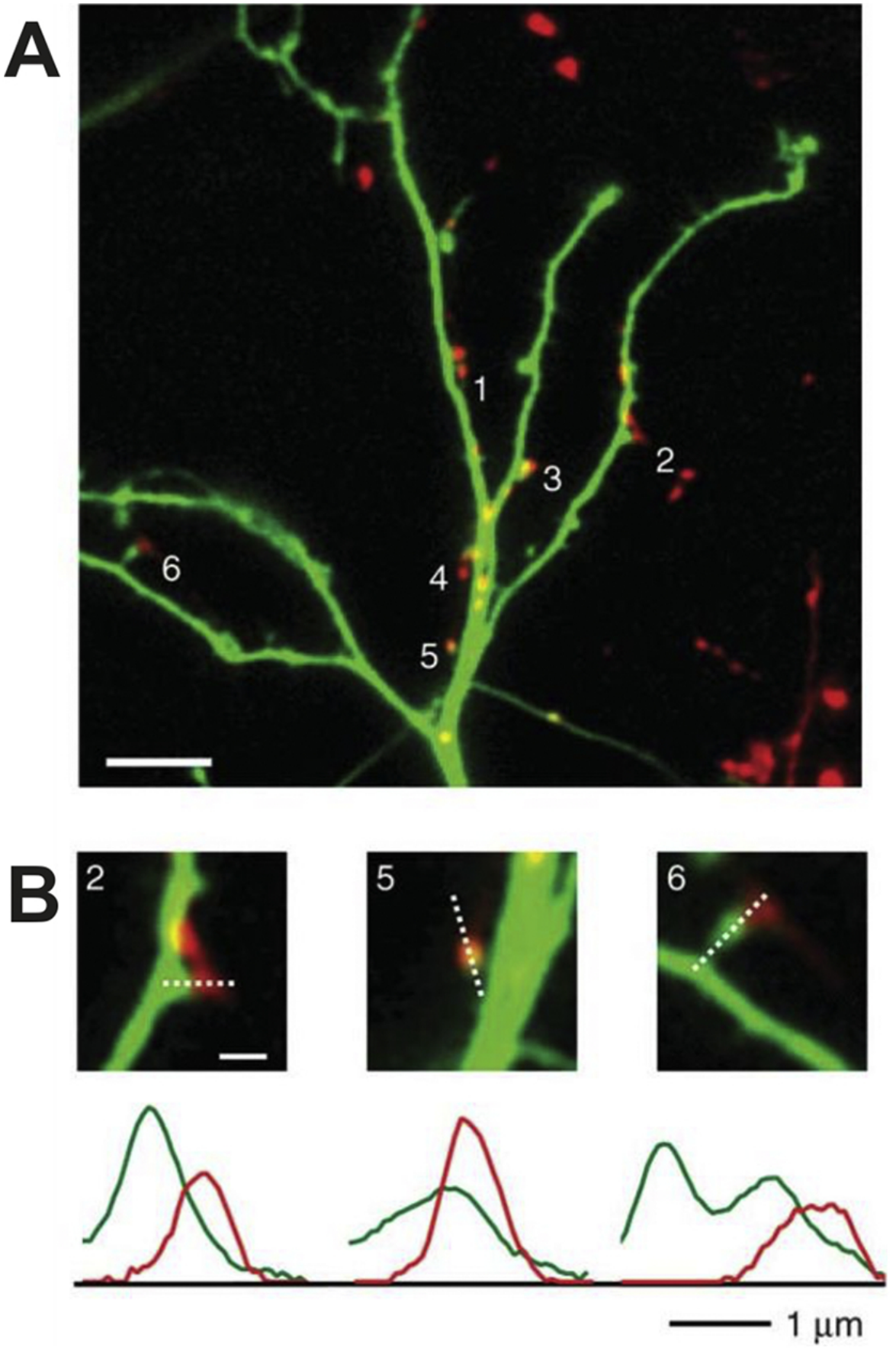

Figure 4

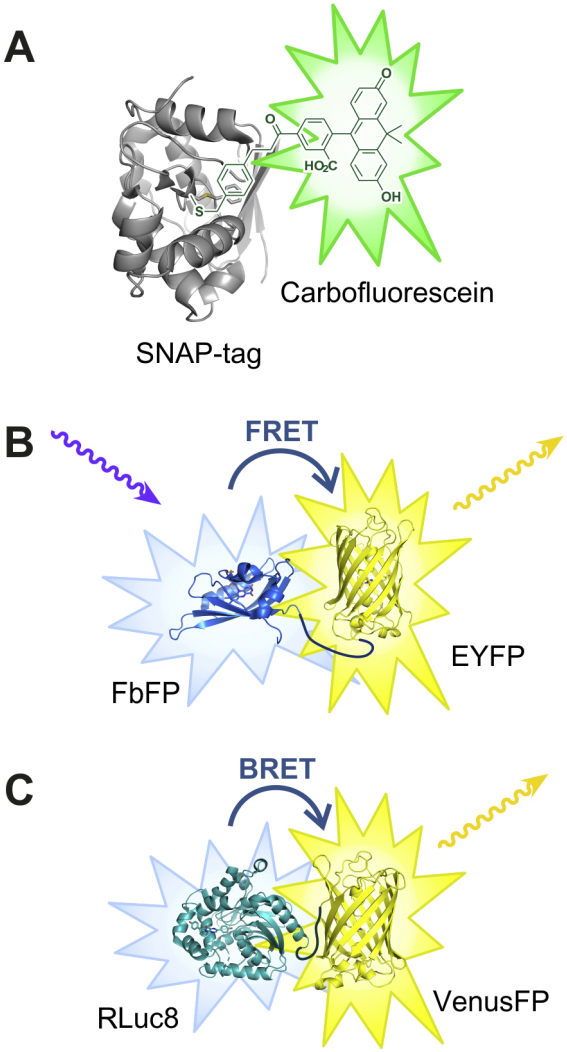
A
O
O
HO2C
OH
S
Carbofluorescein
SNAP-tag
B
FRET
FbFP
EYFP
C
BRET
RLuc8
VenusFP

Figure 5